DOE/ID-22166

Recd
10/2/0

IN SITU PRODUCTION OF CHLORINE-36 IN THE EASTERN SNAKE RIVER PLAIN AQUIFER, IDAHO: IMPLICATIONS FOR DESCRIBING GROUND-WATER CONTAMINATION NEAR A NUCLEAR FACILITY

U.S. GEOLOGICAL SURVEY

Water-Resources Investigations Report 00-4114

Prepared in cooperation with the
U.S. DEPARTMENT OF ENERGY

USGS
science for a changing world

Cover: Rhyolite outcrop at Calamity Creek, Idaho.
Photo by L. D. Cecil, U.S. Geological Survey.

IN SITU PRODUCTION OF CHLORINE-36 IN THE EASTERN SNAKE RIVER PLAIN AQUIFER, IDAHO: IMPLICATIONS FOR DESCRIBING GROUND-WATER CONTAMINATION NEAR A NUCLEAR FACILITY

By L. DeWayne Cecil, LeRoy L. Knobel, and Jaromy R. Green, U.S. Geological Survey, Idaho Falls, Idaho; *and* Shaun K. Frape, University of Waterloo, Ontario, Canada

U.S. GEOLOGICAL SURVEY

Water-Resources Investigations Report 00-4114

Prepared in cooperation with the
U.S. DEPARTMENT OF ENERGY

Idaho Falls, Idaho

2000

U.S. DEPARTMENT OF THE INTERIOR
BRUCE BABBITT, Secretary

U.S. GEOLOGICAL SURVEY
Charles G. Groat, Director

Any use of trade, product, or firm names in this publication is for descriptive purposes only and does not constitute endorsement by the U.S. Government.

For additional information write to:
U.S. Geological Survey
INEEL, MS 4148
P. O. Box 2230
Idaho Falls, ID 83403-2230

Copies of this report can be purchased from:
U.S. Geological Survey
Information Services
Box 25286, Denver Federal Center
Denver, CO 80225-0046

CONTENTS

FIGURES

TABLES

CONVERSION FACTORS AND OTHER ABBREVIATED UNITS

Multiply	By	To obtain
centimeter per year (cm/yr)	0.394	inch per year
cubic centimeter (cm^3)	0.061	cubic inch
gram (g)	0.035	ounce
gram per cubic centimeter (g/cm^3)	0.578	ounce per cubic inch
gram per liter (g/L)	0.133	ounce per gallon
meter (m)	3.281	foot
meter per kilometer (m/km)	5.28	foot per mile
kilogram (kg)	2.204	pound
liter (L)	0.264	gallon
square centimeter per gram (cm^2/g)	4.394	square inch per ounce
square centimeter per second (cm^2/s)	0.155	square inch per second
square kilometer (km^2)	0.386	square mile
square meter per day (m^2/d)	10.76	square foot per day
degree Celsius (°C)	[°C (9/5) + 32]	degree Fahrenheit (°F)

Other abbreviated units used in this report:

MeV (million electron volts)
mg/kg (milligrams per kilogram)
mg/L (milligrams per liter)
mL (milliliters)
$(n/cm^2)/s$ (neutrons per square centimeter per second)
(n/g)/yr (neutrons per gram of rock per year)
ppm (parts per million)
p (proton)
n (neutron)
γ (gamma)
α (alpha particle)
σ (sigma)
μ (muon)
yr^{-1} (per year)

IN SITU PRODUCTION OF CHLORINE-36 IN THE EASTERN SNAKE RIVER PLAIN AQUIFER, IDAHO: IMPLICATIONS FOR DESCRIBING GROUND-WATER CONTAMINATION NEAR A NUCLEAR FACILITY

By L. DeWayne Cecil, LeRoy L. Knobel, *and* Jaromy R. Green, U.S. Geological Survey, Idaho Falls, Idaho; *and* Shaun K. Frape, University of Waterloo, Ontario, Canada

ABSTRACT

In situ chlorine-36 (^{36}Cl) production resulting from nuclear interactions between nonradioactive (stable) nuclides and particles given off during the radioactive transformation of uranium (U) and thorium (Th) decay-series isotopes was determined for 25 whole-rock samples collected from 6 major water-bearing rock types in the eastern Snake River Plain aquifer. The rock types investigated were basalt, rhyolite, limestone, dolomite, shale, and quartzite. Calculated ratios of $^{36}Cl/Cl$ in these rocks, as a result of neutron activation of stable chlorine-35, ranged from 1.4×10^{-15} (basalt) to 45×10^{-15} (rhyolite). The associated neutron production rates calculated for these rock types were 2.5 neutrons per gram of rock per year [(n/g)/yr] for the basalt and 29 (n/g)/yr for the rhyolite. The larger neutron production rate for the rhyolite is due to the larger U (11.5 parts per million, ppm) and Th (22.2 ppm) concentration of the rhyolite; for comparison, the U and Th concentrations of the basalt were 0.8 and 2.23 ppm, respectively.

When the chloride (Cl^-) concentration and rock porosity are considered with the calculated $^{36}Cl/Cl$ ratios, the estimated maximum corrected concentrations of ^{36}Cl in ground water associated with the 6 rock types analyzed in this study ranged from 2.45×10^5 atoms per liter (atoms/L) for ground water in the basalt to 7.68×10^6 atoms/L for ground water in the rhyolite. These values are at least seven orders of magnitude smaller than concentrations measured in ground water at and near the Idaho National Engineering and Environmental Laboratory (INEEL). A ^{36}Cl concentration of $15\pm0.1\times10^{12}$ atoms/L has been reported for a ground-water sample collected near the Idaho Nuclear Technology and Engineering Center, a nuclear-waste processing facility at the INEEL. Additionally, *in situ* $^{36}Cl/Cl$ ratios in ground water from rock with average compositions from this study ranged from 4.0×10^{-15} to 33.3×10^{-15}. For comparison, the range of $^{36}Cl/Cl$ for 254 ground-water samples collected from the Snake River Plain aquifer at and near the INEEL was 31×10^{-15} to 2.9×10^{-9}.

Determining the contribution of *in situ* production to ^{36}Cl inventories in ground water facilitated the identification of the source for this radionuclide in environmental samples. On the basis of calculations reported here, *in situ* production of ^{36}Cl was determined to be insignificant compared to concentrations measured in ground water near buried and injected nuclear waste at the INEEL. Maximum estimated ^{36}Cl concentrations in ground water from *in situ* production are on the same order of magnitude as natural concentrations in meteoric water.

INTRODUCTION

Radioactive chlorine-36 (^{36}Cl) is being measured at extremely small environmental concentrations at and near the Idaho National Engineering and Environmental Laboratory (INEEL) to define the leading edge of a con-

taminant plume that has developed in ground water near this U.S. Department of Energy (DOE) site in southeastern Idaho (fig. 1). The U.S. Geological Survey (USGS), in cooperation with the DOE, has been investigating the hydrologic conditions of the eastern Snake River Plain aquifer over time and space to describe the transport and fate of several contaminants, including tritium (^{3}H), iodine-129 (^{129}I), and ^{36}Cl. To date, ^{36}Cl has proven to be the preferred isotope, compared with ^{3}H or ^{129}I, for describing maximum ground-water flow velocities and first arrival of contaminants at observation wells downgradient from sources at the INEEL (Cecil and others, 1992, 1998, 1999).

To better describe the leading edge of the contaminant plume and the transport and fate of ^{36}Cl in the environment at the INEEL, a more complete understanding of the sources for ^{36}Cl is needed. There are four sources of ^{36}Cl in the eastern Snake River Plain aquifer: (1) natural production by cosmic-ray interaction with argon-40 (^{40}Ar) and neutron activation of argon-36 (^{36}Ar) in the upper atmosphere followed by transportation of the ^{36}Cl through the hydrologic environment as meteoric concentrations in precipitation (Cecil and others, 1999); (2) production by neutron activation of stable chlorine-35 (^{35}Cl) during nuclear-weapons tests of the 1950's and 1960's (Cecil and Vogt, 1997); (3) ^{36}Cl released during nuclear-waste processing at the INEEL (Cecil and others, 1992, 1998, 1999; Beasley and others, 1993); and (4) natural *in situ* production in the aquifer matrix at depth due primarily to neutron activation of stable ^{35}Cl. This report describes the contribution of *in situ* production, in the aquifer matrix at depth, to ^{36}Cl inventories measured in ground water. Meteoric, weapons tests, and nuclear-waste processing contributions to ^{36}Cl inventories in southeastern Idaho are described in other reports (Cecil and others, 1992, 1998, 1999).

Purpose and Scope

The purpose of this report is to describe the calculated contribution to ground water of natural, *in situ* produced ^{36}Cl in the eastern Snake River Plain aquifer and to compare these concentrations in ground water with measured concentrations near a nuclear facility in southeastern Idaho. The scope focused on isotopic and chemical analyses and associated ^{36}Cl *in situ* production calculations on 25 whole-rock samples from 6 major water-bearing rock types present in the eastern Snake River Plain. The rock types investigated were basalt, rhyolite, limestone, dolomite, shale, and quartzite. The calculated contribution included the estimation of neutron production rates based on the elemental composition of the rock samples and the proportion of the resultant neutrons that may be captured by chlorine atoms within the rock to produce ^{36}Cl.

Geohydrology of the Study Area

The eastern Snake River Plain (fig. 1) is a structural downwarp (basin) filled predominantly with Quaternary basalt of the Snake River Group that is generally within 3 m of the land surface (Garabedian, 1992; Whitehead, 1992). This structural basin, defined by faulting and downwarping on the southeast and faulting on the northwest, was created by Cenozoic tectonic stresses and is a zone of transition between the Northern Rocky Mountains and Basin and Range geologic provinces to the north and east and the Basin and Range province to the southeast. Unconsolidated sediments overlie the basin margins and are interbedded with the basalts and pyroclastics at depth. The basalts are several hundred to as much as 1,500 m thick and underlie most of the basin. Fractures and vesicular zones near the surfaces of the basalt flows may be highly transmissive of ground water. Reported transmissivities for the eastern Snake River Plain aquifer range from 0.1 to more than 70,000 m^2/day, a range of nearly six

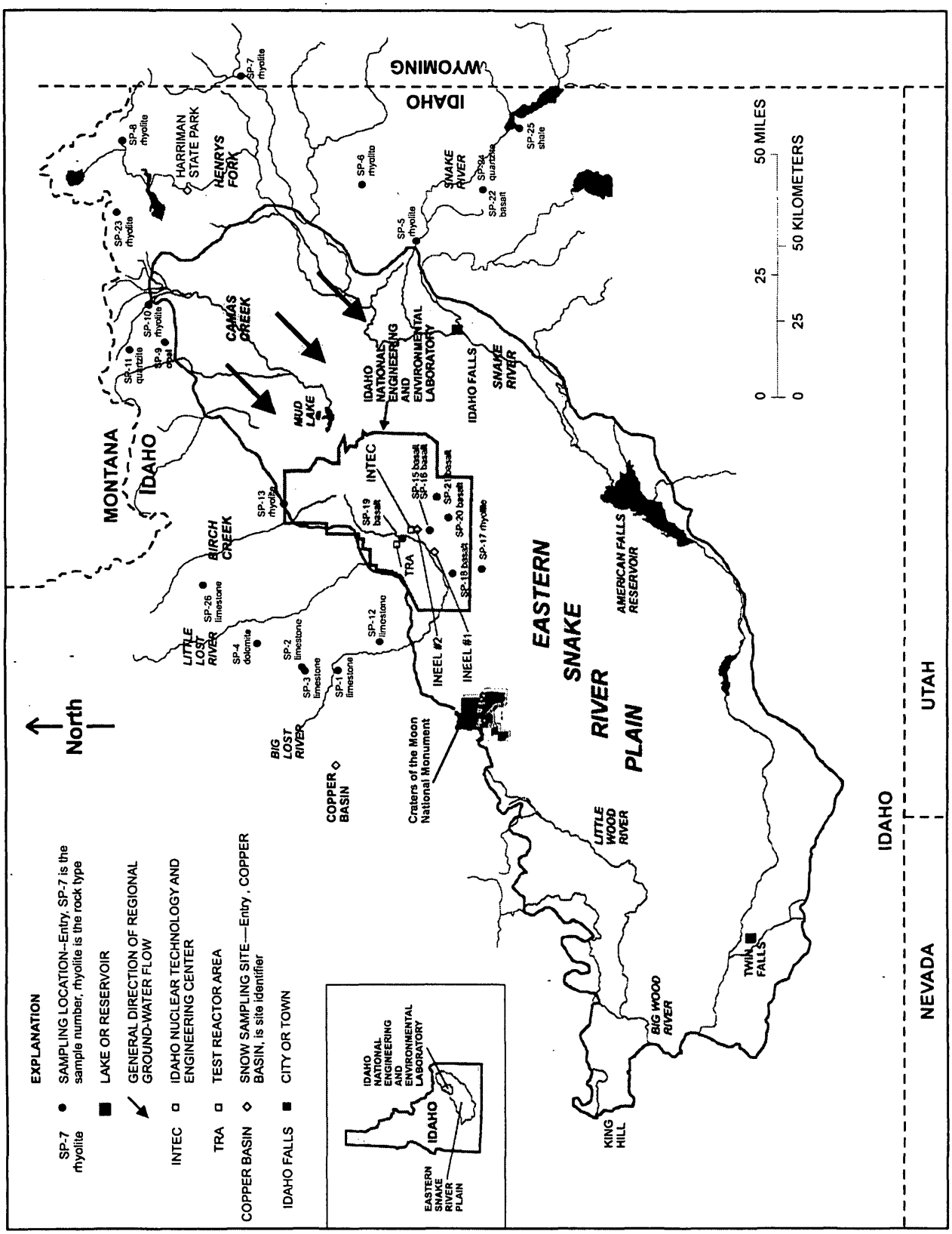

Figure 1. Location of the eastern Snake River Plain, the Idaho National Engineering and Environmental Laboratory, and selected sampling sites.

orders of magnitude (Ackerman, 1991). Depth to water at the INEEL varies in the basalt aquifer from about 60 m below land surface in the northern part to more than 275 m in the southern part. The hydraulic gradient at the INEEL is about 1 m/km, and horizontal linear groundwater flow velocity ranges from 1 to 6 m/day. This range is based on the distribution of ^{36}Cl through time as determined from analyses of archived samples (Cecil and others, in press).

Long-term (1950-88) average precipitation in the vicinity of the INEEL is 22 cm/yr (Clawson and others, 1989, table D-1). About 40 percent of the long-term average precipitation on the eastern Snake River Plain is rainfall between April and September. However, as a result of evapotranspiration, less than 5 percent of the long-term annual average precipitation infiltrates the surface locally on the eastern Snake River Plain (Cecil and others, 1992). As illustrated in the section in this report entitled "Comparison of *in situ* produced chlorine-36 with concentrations in water", evapotranspiration can significantly affect meteoric ^{36}Cl concentrations measured in water from the eastern Snake River Plain aquifer. Recharge to the eastern Snake River Plain aquifer is from snowmelt in the mountains to the east, west, and north, and from irrigation return flow and surface water. The five watersheds that recharge the upper Snake River Plain aquifer are the Big Lost River, Little Lost River, Birch Creek, Camas Creek/Mud Lake, and the main Snake River drainage (fig. 1).

The INEEL comprises about 2,300 km^2 of the eastern Snake River Plain in southeastern Idaho. The INEEL was established in 1949 and is used by the DOE to construct and test nuclear reactors and to participate in various defense programs. Radiochemical and chemical wastes generated at the INEEL and other DOE facilities have been buried at the site since 1952. Additionally, from 1952 to 1984, low-level radioactive and chemical wastes were discharged into the eastern Snake River Plain aquifer at the Idaho Nuclear Technology and Engineering Center (INTEC) through a 182-m-deep disposal well. Since 1984 at the INTEC, and during 1952-93 at the Test Reactor Area (TRA, fig. 1), these wastes also have been discharged to infiltration ponds. The wastewater discharged to ponds at these two facilities must travel through about 150 m of alluvium, sedimentary interbeds, and basalt before reaching the aquifer.

In this report, the solid-phase (rock) samples are designated SP, and their locations are shown on figure 1. In addition, geochemistry of the SP samples is described in tables 1, 2, and 3. The basalt flows that compose most of the Snake River Plain are in layers of only a few meters thick and cover areas of tens to hundreds of square kilometers. Samples SP-15, SP-16, SP-18, SP-19, SP-20, SP-21, and SP-22 are representative of younger basalts on the eastern Snake River Plain (table 1). Large-scale basalt flows, such as those in Oregon and Washington, have not been found in the Snake River Plain. The most recent volcanic eruptions on the Snake River Plain were at the Craters of the Moon National Monument (fig. 1) around 2,000 years ago (Kuntz and others, 1988).

Volcanism produced relatively thick flows of welded tuff, ash, and pumice that are exposed within and near the margins of the basin and are composed largely of rhyolite, latite, and andesite. The rhyolitic tuffs and rhyolite in this group are represented by samples SP-5, SP-6, SP-7, SP-8, SP-9, SP-10, SP-13, SP-17, and SP-23 (table 1). Subsequent basalt volcanism over the entire basin was limited predominately to outpourings of pahoehoe lava (Nace and others, 1975). Some eruptions however, such as the ones near Craters of the Moon, were violent enough to create pyroclastic rocks and significant deposits of cinders. None of these pyroclastic deposits are major aquifers in the basin. Pre-Cretaceous sedimentary and metamorphic rocks border the basin to the northwest and east and are represented in this study by samples SP-1, SP-2, SP-3, SP-4, SP-11, SP-12, SP-24, SP-25, and SP-26 (tables 2 and 3). Of the 6 rock types studied, basalt and rhyolite compose most of the aquifer on the plain, and limestone and dolomite, with minor shale, quartzite, and

medasediments, compose the recharge areas to the north, west, and east.

Acknowledgments

This research was carried out in cooperation with the U.S. Department of Energy. The authors thank David Frederick, Geologist, State of Idaho INEEL Oversight Program; Scott Hughes, Geologist, Idaho State University; and June Fabryka-Martin, Geochemist, Los Alamos National Laboratory, for their critical review. Their many comments and suggestions greatly improved the manuscript.

METHODS

Twenty-five rock samples were submitted to the Idaho State University (ISU), Department of Geology, Geochemical Laboratory for analysis of elemental chemistry. The Geochemical Laboratory prepared samples for analysis by three separate analytical methods: inductively coupled plasma-atomic emission spectrometry (ICP-AES), instrumental neutron activation analysis (INAA), and loss on ignition (LOI). In addition, selected solid-phase samples were submitted to the USGS Branch of Geochemistry Laboratory to determine Cl^- concentration by ion-selective electrode potentiometry (ISEP). The data were received from the two laboratories and were processed into the form needed to make *in situ* production calculations for ^{36}Cl. The processed data needed for the calculations are presented in tables 1, 2, and 3.

Field Methods

For the *in situ* ^{36}Cl production calculations, it was assumed that the dominant mechanism of production was neutron activation of stable ^{35}Cl. At depths greater than about 10 m in most rocks, this assumption holds (Gifford and others, 1985, p. 418; Fabryka-Martin, 1988, tables h-3a through h-3h). Although some of the whole-rock samples collected for this study were from the upper 2 to 5 m of the rock formation at land surface and may have undergone some changes as a result of weathering, the chemical data presented in tables 1, 2, and 3 are assumed to be representative of the entire depth of the rock type, both temporally and spatially. For basalt and rhyolite samples SP-15 through SP-21 (table 1), the depth of collection was greater than 50 m in all cases; these samples were extracted from rock cores housed in the USGS Lithologic Core Library at the INEEL. All whole-rock samples were collected from fresh exposures or cores using standard methods and powderless gloves to minimize contamination.

Analytical Methods

Sample processing for each of these analytical methods began with the preparation of a homogeneous powdered sample. Each powdered sample subsequently underwent processing according to the specific analytical method to be applied. Additionally, rock samples sent to the ISU Geochemical Laboratory for analyses were further processed to insure that unweathered samples were used for all analyses.

Inductively coupled plasma-atomic emission spectroscopy (ICP-AES)

For analyses by ICP-AES, the sample must be prepared as a solution (Lichte and others, 1987). There are a variety of methods to prepare the solution and each method has advantages that are related to sample composition. Sequential acid dissolution using hydrofluoric acid (HF), aqua regia, perchloric acid ($HClO_4$), and nitric acid (HNO_3) is one procedure that has the disadvantage that silicon and boron are lost because of their volatility as fluorides. Several trace minerals, including chromite, are not completely dissolved by this procedure. Because of the silicic composition of volcanic rocks in the Snake River Plain, a fusion method of preparing sample solutions was used by the ISU laboratory as opposed to the sequential acid dissolution method.

The fusion method uses a flux to convert the sample to a glass bead, which subsequently is dissolved in dilute HNO_3 to prepare a solution for analysis. The specific procedure used by the ISU Geochemical Laboratory involved mixing 0.1 g of powdered sample and 0.3 g of lithium metaborate in a graphite crucible and heating in a furnace for 20 minutes at 1,050 °C. The con-

tents of the crucible were poured immediately into 75 mL of 3.5-percent HNO_3 in a 250-mL beaker and stirred on a magnetic stirrer for 5 minutes or until the sample was clear. The contents of the beaker then were transferred to a 100-mL volumetric flask, and more dilute HNO_3 was added to bring the volume to 100 mL. The flask was capped and gently shaken to thoroughly mix the contents. A sample bottle was pretreated by rinsing with 5 mL of the sample solution that then was discarded. The pretreated sample bottle then was filled with 50 mL of the sample solution and was ready for analysis by ICP-AES. The ISU laboratory reported weight percent values for oxides of the following elements: silicon, titanium, aluminum, manganese, magnesium, calcium, potassium, and phosphorus. Using this method, the laboratory also determined strontium, zirconium, and yttrium concentrations in units of parts per million (ppm) by weight.

Instrumental neutron activation analysis (INAA)

For analyses by INAA, a precisely known amount of powdered sample must be prepared to undergo irradiation without the loss of sample (Baedecker and McKown, 1987). The laboratory placed 1 g or less, weighed to the nearest milligram, into a 0.4-dram, reactor-safe, laboratory-grade polyvial, which then was heat sealed. The 0.4-dram polyvial then was heat sealed into a 2-dram, reactor-safe, laboratory-grade polyvial. Preparation for neutron activation then was complete. For calibration purposes, three reference standards were included with the samples: USGS rock standards BCR-1 and BHVO-1 and the National Institute of Science and Technology (NIST) traceable coal fly ash standard reference material (SRM) 1633-A.

The prepared standards and samples were sent to the Oregon State University (OSU) Radiation Center for neutron activation in the TRIGA Reactor. Neutron activation lasted 2 hours under a neutron flux of 3×10^{12} $(n/cm^2)/s$. Once activated, the standards and samples were returned to ISU for analysis. Upon arrival at the laboratory, the inner 0.4-dram polyvials were transferred into new 2-dram polyvials for gamma counting.

Activation analysis is based on measurement of activity from radioactive nuclides produced by nuclear reactions on naturally occurring isotopes of the sample elements during the activation process. Gamma-ray spectroscopy at the ISU Geochemical Laboratory employed semiconductor detectors (high-purity germanium diodes) for gamma counting. These devices converted a gamma-ray signal from the irradiated samples to electronic pulses that could be sorted and processed by a multichannel analyzer and supporting electronics. The resulting spectra then were processed by computer software and the results were recorded. All standards and samples were counted three separate times in a sequence that optimized peak-to-background ratios for short-, intermediate-, and long-lived radionuclides, respectively. The first counts were for determining the short-lived radionuclides of sodium, samarium, lanthanum, and uranium (U), and took place about 5 days after irradiation. The count periods were between 2,000 and 4,000 seconds. The next counts were for the intermediate-lived radionuclides of barium, rubidium, neodymium, ytterbium, and lutetium, and took place about 10 to 20 days after irradiation. The count periods were 8,000 to 10,000 seconds. The final counts were for the long-lived radionuclides of iron, scandium, chromium, nickel, cobalt, cesium, cerium, europium, terbium, thorium (Th), hafnium, and tantalum, and took place about 30 to 40 days after irradiation. The count periods were 20,000 to 40,000 seconds. Results were reported in ppm by weight, except for sodium and iron, which were reported as oxides of the elements in weight percent.

Loss on ignition (LOI)

For analysis by LOI at the ISU Geochemical Laboratory, precisely 2 g of powdered sample weighed to within 0.0005 gram were placed in a clean ceramic crucible. The weight of the crucible and powder was determined and recorded. The open crucibles were heated overnight (or for about 12 hours) at 90°C. The crucibles were removed to a desiccator, cooled for 2 to 3 min-

utes and reweighed. These raw weights were recorded and subtracted from the weights of the unheated crucibles and powdered sample. The difference represented the weight of volatile components that are not actually part of the sample. The samples were returned to a desiccator and a muffle furnace was heated to 950°C. When the muffle furnace reached this temperature, lids were placed on the crucibles and they were heated for 1 hour. The crucibles were cooled 2 minutes, then the lids were removed and the crucibles were allowed to continue cooling in the desiccator until they reached room temperature (about 5 to 7 minutes). After cooling, the weights of the crucibles were determined and subtracted from the raw weight of the crucible and sample determined previously. The weight difference in grams represented the LOI component of the sample. The difference was divided by the original sample weight (2±0.0005 g) and multiplied by 100. This value was reported along with the elemental oxides as LOI in weight percent.

Ion-selective electrode potentiometry (ISEP)

For analysis of Cl^- by ISEP, 200 mg of powdered sample were weighed and placed into a confined area of the outer compartment of a Conway diffusion cell constructed of Teflon (Aruscavage, 1990). Oxidizing and reducing solutions were prepared. The reducing solution was made of 22.6 g of potassium hydroxide (KOH) dissolved in 140 mL of deionized water (H_2O) and 1.12 g of anhydrous sodium sulfite (Na_2SO_3). A 2.5-mL aliquot of reducing solution was pipetted into the inner compartment of the Conway diffusion cell. The oxidizing solution was made of 160 mL of HF added to a solution that contained 2.6 g of potassium permanganate ($KMnO_4$) dissolved in 50 mL of 15-percent sulfuric acid (H_2SO_4). A 3-mL aliquot of the oxidizing solution was added to the outer compartment of the Conway diffusion cell and digested the powdered sample by mixing overnight on an oscillating platform. The evolved chlorine was converted to Cl^- by the reducing solution contained in the inner compartment of the Conway diffusion cell. Finally, the Cl^- concentration was measured by ISEP. The applicable concentration range for Cl^- by this method was 0.01 to 2.00 percent by weight, or 100 to 20,000 ppm by weight.

Data Processing

The methods used to determine the maximum *in situ* produced atom concentrations for ^{36}Cl in ground water have been documented in reports by Fabryka-Martin (1988) and Andrews and others (1989) and are discussed in the section titled "*In situ* production of chlorine-36." Geochemical data for the rock samples generated by contract laboratories and used in this report were converted for use in the necessary *in situ* production calculations using the ion-specific methods described in the following sections.

Chloride

Results generated by the USGS Branch of Geochemistry were reported as percent by weight Cl^- with a reporting level of 0.01 percent. These numbers were converted directly to ppm by weight using the following equation:

$$(\text{weight percent } Cl^-/100)\times 1{,}000{,}000 \text{ g} = \text{ppm by weight } Cl^-. \quad (1)$$

For example,

$$(0.04 \text{ weight percent } Cl^-/100)\times 1{,}000{,}000 \text{ g} = 400 \text{ ppm } Cl^-.$$

Fourteen solid-phase samples were selected for determination of Cl^- concentration. For the 11 of 14 Cl^- results that were larger than the laboratory reporting level, the converted results were used directly in tables 1, 2, and 3. The Cl^- concentrations for the three samples that were determined to be less than the laboratory reporting level and for the samples that were not analyzed for Cl^- (marked with an asterisk in tables 1, 2, and 3) were taken from a report by Parker (1967, table 19, p. D13-D14).

Gadolinium

Gadolinium has the largest neutron absorption cross section (49,000 barns/atom, table 4) of all major and trace elements used in the *in situ* calculations. Therefore, the determination

of gadolinium in the rocks of the eastern Snake River Plain was essential for determining the total cross section of the rock for thermal neutron absorption.

The ISU Geochemical Laboratory reported concentrations of samarium and terbium directly in ppm; however, the laboratory did not determine gadolinium. Because gadolinium concentrations were needed to calculate *in situ* production of ^{36}Cl, and because the relation between concentrations of samarium, terbium, and gadolinium in chondritic meteorites and terrestrial materials is systematic, the relation between these three elements in chondritic meteorites and the measured concentrations of samarium and terbium in the samples were used to estimate gadolinium concentrations by interpolation. The gadolinium concentrations were calculated by normalizing measured concentrations of samarium and terbium to their nonvolatile mass concentrations in carbonaceous chondritic meteorites (designated the C1-chondrite) using values tabulated by Anders and Ebihara (1982, table 1). The values from Anders and Ebihara first were converted to nonvolatile mass concentrations by subtracting volatile elements from the total, then renormalizing to 100 percent. This process yielded appropriate values to which terrestrial samples were normalized using the following equations (Scott Hughes, ISU, written commun., 1999):

$$(Sm\text{-}N) = (Sm)/0.197, \text{ and} \quad (2)$$

$$(Tb\text{-}N) = (Tb)/0.047, \quad (3)$$

where

(Sm-N) = Cl-chondrite normalized concentration of samarium;

(Sm) = measured concentration of samarium, in ppm;

0.197 = Cl-chondrite total mass for samarium converted to nonvolatile mass, in ppm;

(Tb-N) = Cl-chondrite normalized concentration of terbium;

(Tb) = measured concentration of terbium, in ppm; and

0.047 = Cl-chondrite total mass for terbium converted to nonvolatile mass, in ppm.

The normalized concentrations of samarium and terbium then were used to calculate the normalized concentration of gadolinium:

$$(Gd\text{-}N) = 10^{[\log(Sm\text{-}N) + 2\log(Tb\text{-}N)]/3}, \quad (4)$$

where

(Gd-N) = Cl-chondrite normalized concentration of gadolinium.

Finally, the normalized gadolinium concentrations were converted to the estimated gadolinium concentrations shown in tables 1-3 using the following equation:

$$(Gd) = 0.26(Gd\text{-}N), \quad (5)$$

where

(Gd) = calculated concentration of gadolinium, in ppm; and

0.26 = Cl-chondrite total mass for gadolinium converted to nonvolatile mass, in ppm.

The estimated gadolinium concentrations were evaluated by applying this method to an independent data set that contained measured concentrations of samarium, terbium, and gadolinium in 56 basalt samples from the eastern Snake River Plain (Knobel and others, 1995). The measured samarium and terbium concentrations were used to estimate gadolinium concentrations by means of equations 2 through 5. The estimated gadolinium concentrations were individually compared to the measured gadolinium concentrations to determine the percent differences of the estimated concentration relative to the measured concentration for all 56 samples. All 56 estimated gadolinium concentrations were within 25 percent of the measured concentrations: 51 were within 15 percent, and 47 were within 10 percent.

Mean concentrations of the measured and estimated data sets were calculated along with the estimated uncertainties of the mean concentrations. The mean and the associated uncertainty for the mean of the measured gadolinium data set was 7.7±1.8 ppm and 7.3±1.7 ppm for the estimated gadolinium data set (table 5). The good agreement between the means of the two data sets suggests that gadolinium concentra-

tions estimated using equations 2 through 5 are reasonable approximations of the true measured concentrations.

Another means of testing the acceptability of the estimated gadolinium concentrations is to plot the laboratory-measured results with the estimated gadolinium concentrations. If equations 2 through 5 produce exact estimates of the measured gadolinium concentrations, a straight line with a slope of 1 and a y-intercept of 0 should result. The data are plotted on figure 2 and a linear regression analysis gives a straight line with a slope of 0.87 and a y-intercept of 0.59. The correlation coefficient is 0.91, which suggests an acceptable match between the measured and estimated gadolinium concentrations. These comparisons suggest that equations 2 through 5 provide acceptable estimates of gadolinium concentrations in rocks from the eastern Snake River Plain aquifer system.

Lithium, beryllium, boron, carbon, and fluorine

The ISU Geochemical Laboratory did not measure the concentrations of these light elements in the samples as listed in tables 1, 2, and 3. Because these elements were needed for the calculation of *in situ* ^{36}Cl production, concentrations equivalent to average concentrations in the appropriate sample rock type were included in this analysis. These concentrations were taken from Parker's study (1967, table 19, p. D13-D14) and were marked with asterisks in tables 1, 2, and 3. Carbon (C) concentrations in tables 1, 2, and 3 not marked with an asterisk were calculated using other methods. Those methods will be discussed in the sections entitled "Carbonate sedimentary rocks" and "Noncarbonate sedimentary and metamorphic rocks."

Boron has the largest absorption cross section of these five elements, 764 barns/atom, and so has the potential to significantly affect the overall thermal neutron cross section, depending on the boron concentration in the sample (table 4). Therefore, a sensitivity analysis was performed on the samples to determine the effect of various boron concentrations on the $^{36}Cl/Cl$ ratio. Average boron concentrations taken from Parker's study ranged from 5 ppm for basalt to as much as 100 ppm for shale. A smaller boron concentration in a sample generally corresponds to a larger $^{36}Cl/Cl$ ratio because more of the neutron flux is available for activation of ^{35}Cl. Therefore, the sensitivity analysis was performed under the assumption that the average boron concentrations were lower by an order of magnitude.

The largest percent change in $^{36}Cl/Cl$ ratios was for sample SP-24, a quartzite. The calculated $^{36}Cl/Cl$ ratio using an average boron concentration for quartzite taken from Parker's study (1967) was 1.5×10^{-15}, and the $^{36}Cl/Cl$ ratio adjusted for a smaller boron concentration was 2.5×10^{-15}, or a 61-percent increase. The smallest percent change in $^{36}Cl/Cl$ ratios was for sample SP-20, a basalt. The calculated $^{36}Cl/Cl$ ratio was 1.4×10^{-15}, and the adjusted $^{36}Cl/Cl$ ratio was 1.5×10^{-15}, or an increase of only 0.7 percent. None of the ratios for the basalt samples changed by greater than 2.7 percent as a result of this change in boron concentration. Ratios for the rhyolite samples, with the exception of SP-9, changed 8.6 percent or less. Ratios for the carbonate, opal, shale, and quartzite samples all changed at least 20 percent. The average increases in $^{36}Cl/Cl$ ratios for the basalt and rhyolite samples were 2.3 and 7.5 percent, respectively. The average increases in $^{36}Cl/Cl$ ratios for the carbonate, opal, shale, and quartzite samples were 25, 24, 46, and 42 percent, respectively. The larger increase in the $^{36}Cl/Cl$ ratios for these samples was due to the decrease in boron concentration in the samples. The order of magnitude decrease in the boron concentration increased the thermal neutron cross section

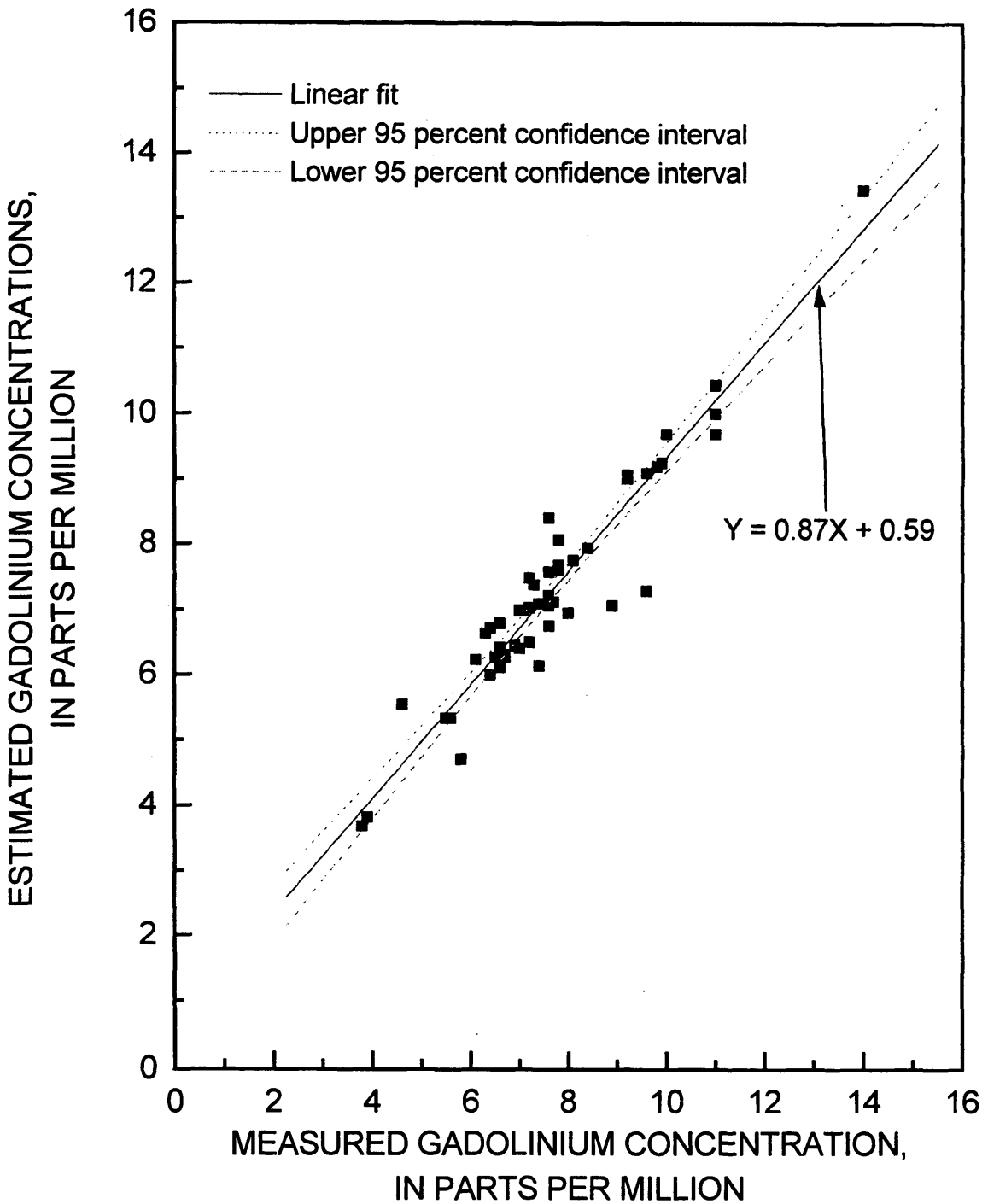

Figure 2. Measured and estimated gadolinium concentrations for 56 basalt samples from the eastern Snake River Plain.

available for ^{35}Cl activation and, hence, increased the $^{36}Cl/Cl$ ratio.

As an example, there was a 46-percent change in the $^{36}Cl/Cl$ ratio for the shale sample (boron concentration = 10 ppm) that was 20 times greater than the 2.3-percent ratio change for the average basalt sample (boron concentration = 0.5 ppm). Thus, the change in the $^{36}Cl/Cl$ ratio for the shale sample as a result of the order of magnitude decrease in the boron concentration was significant compared to the change in this ratio for basalt samples with a corresponding change in boron concentrations. However, as mentioned earlier, the contribution of ^{36}Cl to ground water from shale is insignificant compared to the contribution from basalt because most of the aquifer on the plain is composed of basalt.

The difference in initial boron concentrations for the rock samples also affected the outcome of the sensitivity analysis. For example, the average boron concentration for rhyolite changed from 15 to 1.5 ppm. The average boron concentration for basalt changed from 5 to 0.5 ppm. Although all values decreased by an order of magnitude, the rhyolite samples were affected more by the decrease in boron concentration than the basalt samples were. The average change in boron concentrations for the rhyolite samples was 13.5 ppm, and the average change in boron for the basalt samples was 4.5 ppm. The resultant change in $^{36}Cl/Cl$ ratio was consequently 7.5 percent for rhyolite and only 2.3 percent for basalt.

Regardless of the initial boron concentrations used in this sensitivity analysis, the gadolinium concentrations ultimately determined the degree of effect that the boron concentrations had on the resultant $^{36}Cl/Cl$ ratio. With a gadolinium concentration of 10 ppm, the change in the boron concentration had little or no effect on the $^{36}Cl/Cl$ ratio because gadolinium has such a large absorption cross section compared to that of boron: 49,000 barns/atom for gadolinium and 764 barns/atom for boron. Alternatively, if the gadolinium concentration is 0.01 ppm, the gadolinium will have very little effect on the $^{36}Cl/Cl$ ratio, enabling a change in boron concentration to have a significant effect.

Samarium, terbium, uranium, and thorium

Concentrations of samarium, terbium, uranium, and thorium in tables 1, 2, and 3 were the concentrations reported directly in ppm by the laboratory.

Elements reported as oxides

The laboratory reported the principal rock-forming elements as oxides in weight percent of the total sample weight. The ICP-AES and INAA analytical methods used by the ISU laboratory did not account for the volatile components in the sample; for example, water (H_2O) and carbon dioxide (CO_2). These constituents were measured using the LOI method, which provided a gross estimate of the total volatile fraction of the sample but did not distinguish between the component parts. The weight percent of the LOI fraction of the sample, added to weight percents of the major rock-forming elements, should equal 100 percent. However, a total of 100 percent is rarely obtained, because the LOI method of reporting results does not account for the trace-element content of the rock samples. Because selected trace elements were considered in this report, the laboratory data were not normalized to 100 percent prior to conversion to ppm. Estimation of the volatile components of the sample required additional calculations as discussed in the section "Volatile components."

The principal rock-forming elements are silicon (Si), aluminum (Al), iron (Fe), calcium (Ca), magnesium (Mg), sodium (Na), potassium (K), phosphorus (P), titanium (Ti), and manganese (Mn); the respective oxides are SiO_2, Al_2O_3, FeO, CaO, MgO, Na_2O, K_2O, P_2O_5, TiO_2, and MnO. (Some Fe_2O_3 does exist along with the FeO, but the quantity is small enough that the laboratory reported the total Fe concentration as FeO). Oxygen (O), which is reported as part of the oxides, also is considered a principal

rock-forming element. The weight percent of each oxide was converted to the needed units of ppm by weight by reducing the weight percent to a ratio and multiplying it by 1,000,000 g:

(weight percent oxide/100) × 1,000,000 g = ppm by weight oxide. (6)

The oxide in ppm by weight then was multiplied by the ratio of the elemental weight to the molecular weight of the oxide:

ppm by weight oxide × (elemental weight/molecular weight oxide) = ppm by weight element. (7)

The ppm by weight of O in the oxide was determined by subtracting the ppm by weight of the element from the oxide:

ppm by weight oxide - ppm by weight element = ppm by weight O. (8)

For example, the reported weight percent of SiO_2 for sample SP-15 of 45 used with the known elemental weight of Si (28.1 g) and molecular weight of SiO_2 (60.1 g) gave the following:

(1) From equation 6:
(45/100) × 1,000,000 g = 450,000 ppm by weight SiO_2.

(2) From equation 7:
450,000 × (28.086/60.0848) = 210,348 ppm by weight Si.

(3) From equation 8:
450,000 - 210,348 = 239,652 ppm by weight O.

The ppm by weight of each element was calculated from the appropriate oxide and the results are listed in tables 1, 2, and 3. The ppm by weight of the element O for each oxide was summed and is listed in tables 1, 2, and 3 as oxygen, rock (O,r).

Volatile components

The principal volatile components of the rock samples submitted for analysis were CO_2 and H_2O. The importance of these two compounds in a sample depended on the amount of mineral material containing these compounds that was present in the samples. For example, the laboratory analyzes calcite ($CaCO_3$) in rock as CaO and CO_2, however, CO_2 is included as an undifferentiated component of the LOI result for the sample. Similarly, opal ($SiO_2 \cdot nH_2O$) in rock is analyzed as SiO_2 and H_2O in the laboratory with the H_2O included in the LOI result. Because LOI was undifferentiated, it was necessary to make some assumptions about its content, and these assumptions were made on the basis of the typical mineralogy of the type of rock sample that was submitted for analysis. Also, because LOI was measured with a different analytical method than the oxides were measured, any adjustment necessary to make the ppm by weight values equal 1,000,000 ppm was made in the volatile component of the analysis. Because these assumptions and the resulting calculations depend on the rock type, they will be discussed in that way.

Basalt and rhyolite

The extreme heat associated with the formation of basalt and rhyolite generally drives off most volatile components. Many surface samples of Snake River Plain basalt have coatings and void fillings of caliche, a mixture of calcite and clay that has been deposited by secondary moisture-related processes. In this case, LOI firing can remove CO_2 as a volatile, just like H_2O. However, the basalt samples in this study, with the exception of one sample, were taken from depth where the major sources of CO_2, caliche, and $CaCO_3$, are assumed to be minimal. Therefore, all the LOI for basalt and rhyolite in this study was assumed to be from H_2O and not CO_2. Some H_2O is trapped in vesicles as these rock types solidify from the molten magma and hydration of some minerals takes place. Because of these characteristics, the assumption was made that the difference in table 1 between the raw total (the sum of previously discussed elements) and the adjusted (adj.) total was the result of H_2O lost during the analytical process. The ppm by weight oxide (H_2O) was calculated by subtracting the total raw values from the total adjusted values. Equations (7) and (8) then were used to calculate H and O. These values were designated H,w and O,w and listed in table 1. Calculations for the sample from an opal deposit in rhyolite, SP-9, are discussed in the

section titled "Noncarbonate sedimentary and metamorphic rocks."

Carbonate sedimentary rocks

The idealized chemical formulas for carbonate rocks are $CaCO_3$ (limestone) and $CaMg(CO_3)_2$ (dolomite). The principal volatile component in both rocks is CO_2, and it was assumed in this report that the LOI component of the carbonate samples was the result of CO_2 volatilization. For example, dolomite undergoes a two-stage volatilization:

(1) $CaMg(CO_3)_2 \rightarrow CaCO_3 + MgO + CO_2$ at about 800°C, and

(2) $CaCO_3 \rightarrow CaO + CO_2$ at about 900°C.

The LOI values were converted to ppm by weight of the oxide using equation (6). The remaining calculations were completed using equations (7) and (8). The calculated results for C are listed in table 2 and the O values were included in the summation represented in table 2 by O,r. The H,w and O,w values in table 2 were calculated in the same manner as for the basalt and rhyolite samples in table 1.

Noncarbonate sedimentary and metamorphic rocks

The amount of carbonate minerals in predominantly noncarbonate sedimentary rock is variable and often is mirrored after the sum of calcium and magnesium contained in the rock. For example, a predominantly silica sand may contain grains of calcite and dolomite that have not been removed by weathering processes. Conversely, opal, which is the weathering product of some igneous rocks, should not contain much carbonate material but should contain significant amounts of water.

Calcium and magnesium in clay and shale generally are in the lattice of the complex aluminosilicate minerals contained in clay, and the presence of carbonate minerals should be limited in most cases. On the other hand, clay minerals commonly contain significant quantities of water. The average ppm by weight of carbon in clay and shale was taken from Parker's study (1967, table 19) to represent the value listed in table 2 for sample SP-25. The corresponding oxygen value was calculated by first converting the element ppm by weight to the number of moles of the element. This conversion was accomplished by dividing the elemental mass in grams by the elemental gram formula weight (gfw):

$$element_{ppm}/element_{gfw} = element_{moles} \quad (9)$$

For example, the ppm by weight for carbon in SP-25 is 10,000 g and the moles of C are calculated with equation (9) as follows:

10,000g/12.01115 g/mole = 832.56 moles.

The chemical formula for CO_2 requires two moles of O for each mole of C (2×832.56 moles C) = 1,665.12 moles O. Equation (9) was modified to calculate the ppm by weight value for oxygen.

$$element_{ppm} = element_{moles} \times element_{gfw}$$

Therefore, O ppm by weight in grams = 1,665.12 moles × 15.9994 g/mole = 26,641 g of O. This oxygen number was included in the sum of O listed as O,r in table 2 for sample SP-25.

For the opal sample (SP-9) and the two quartzite samples (SP-11 and SP-24), the assumption was made that the number of moles of C was equal to the sum of the number of moles of calcium and magnesium. Equation (9) was used to calculate the number of moles of calcium and magnesium. The ppm by weight of C was calculated by using equation (8). The results are listed in tables 1 and 3. Once the moles of carbon were known, the moles of oxygen were given by the relation $O_{moles} = (2)(C_{moles})$. The ppm by weight of O was calculated with equation (8) and summed into the appropriate O,r results listed in tables 1 and 3. The H,w and O,w values in tables 1 and 3 were calculated the same way as for the basalt and rhyolite samples.

Anomalous data

Silica weight percents for samples SP-17 and SP-24 were outside the calibration range of the analytical instrument at the time the samples

were analyzed, giving results that were larger than possible. Consequently, these two values were reduced so that the laboratory weight-percent totals equaled 100 percent.

The LOI weight percents for samples SP-16, SP-18, SP-19, SP-20, and SP-21 were reported as negative values because of analytical interferences by iron in the samples. These values were adjusted so that the total (adj) value equaled 1,000,000 ppm by weight.

IN SITU PRODUCTION OF CHLORINE-36

Four potential sources for ^{36}Cl in ground water are (1) meteoric input of cosmogenically-produced ^{36}Cl through wet and dry deposition, 2) *in situ* production by neutron activation in the aquifer matrix or water, (3) radioactive fallout from atmospheric nuclear-weapons tests, and (4) emissions from nuclear-reactor facilities. Chlorine-36, a beta-particle emitter, is cosmogenically produced in the atmosphere by two major processes: (1) spallation (cosmic-ray interaction with ^{40}Ar), and (2) neutron activation of ^{36}Ar according to the following reactions (Andrews and Fontes, 1992):

^{40}Ar (p, n, α) ^{36}Cl (67 percent of total natural atmospheric production), and

^{36}Ar (n, p) ^{36}Cl (33 percent of total natural atmospheric production).

Another significant source of ^{36}Cl in the environment is the neutron activation of stable ^{35}Cl:

$$^{35}Cl\ (n, \gamma)\ ^{36}Cl.$$

This reaction is the source of ^{36}Cl produced during atmospheric weapons tests conducted by the United States and Great Britain over the Pacific Ocean during 1952-58 (Schaeffer and others, 1960). This reaction also may produce significant ^{36}Cl *in situ* in certain subsurface environments that have a neutron source in reasonably close proximity to stable ^{35}Cl. In basalt, rhyolite, sandstone, and carbonate rocks, the following reactions on potassium-39 (^{39}K) and to a lesser extent, on calcium-40 (^{40}Ca), can contribute to *in situ* production:

$$^{39}K\ (n, \alpha)\ ^{36}Cl, \text{ and}$$

$$^{40}Ca\ (\mu, \alpha)^{36}Cl.$$

However, the ^{35}Cl (n, γ)^{36}Cl reaction is the only one that produces significant ^{36}Cl in the subsurface at a depth greater than about 10 m (Andrews and others, 1989; Davis and others, 1998; Fabryka-Martin, 1988).

Calculations were restricted to the deep subsurface (greater than 10 m), under the assumption of rock-unit geochemical homogeneity. Shallow subsurface contributions of ^{36}Cl were assumed to be minimal because seasonal ground-water recharge moves rapidly through the shallow subsurface and precludes the addition of significant ^{36}Cl from near-surface production reactions. Additionally, evapotranspiration on the eastern Snake River Plain is large and resultant long-term regional areal recharge is small, limiting the amount of ^{36}Cl that recharge can mobilize in the near-surface environment (Cecil and others, 1992).

To further support the assumption that ^{36}Cl production resulting from the neutron activation of ^{39}K is negligible, *in situ* secular equilibrium $^{36}Cl/Cl$ ratios resulting from the reaction $^{39}K(n,\alpha)^{36}Cl$ and $^{35}Cl(n,\gamma)^{36}Cl$ were calculated for each of the 25 rock samples in this study (table 6). The ratios resulting from the activation of ^{39}K ranged from 1×10^{-21} to 5×10^{-17}, or three to six orders of magnitude smaller than the ratios resulting from the activation of ^{35}Cl. Thus, the production of ^{36}Cl due to ^{39}K is negligible, and because muon activation of ^{40}Ca yields an even smaller ^{36}Cl production rate, these production mechanisms are insignificant compared to the neutron activation of ^{35}Cl.

The neutrons required for activation of ^{35}Cl and ^{39}K are produced by the interaction between alpha (α) particles, generated from the radioactive decay of U and Th series isotopes, and stable nuclei of lighter elements such as O, Na, Al, and Si (Faure, 1986). An estimate can be made of *in situ* produced ^{36}Cl for a given ground-

water system if the following contributing factors are known: (1) the U and Th content of the aquifer matrix, (2) the concentrations of target elements for (α, n) reactions, (3) the concentration of target elements for neutron capture, and 4) the proximity of target elements to neutrons. Because of the heterogeneous nature of the eastern Snake River Plain aquifer, the proximity of target elements was not determined. Therefore, maximum equilibrium concentrations reported here for ^{36}Cl in ground water were calculated with the assumption that all *in situ* produced atoms in the aquifer matrix were transferred to the fluids flowing through the aquifer. These maximum ^{36}Cl concentrations were used to determine the associated total Cl^- concentration transferred to the ground water.

Additionally, for the calculations of *in situ* produced ^{36}Cl, the following assumptions were made: (1) all neutrons were thermalized in all rocks below about 10 m in depth; (2) thermal neutron fluxes were directly proportional to neutron production rates; (3) all the U and Th decay series isotopes were in secular equilibrium and were homogeneously distributed throughout the rock; (4) all target nuclides were homogeneously distributed throughout the rock; and (5) all rocks were saturated with water. The thermal neutron flux and ^{36}Cl production are reduced in unsaturated rock as a result of neutron capture by other elements in addition to the ^{35}Cl and ^{39}K in the aquifer matrix. Therefore, *in situ* production in the deep unsaturated zone will be reduced by as much as 70 percent compared to *in situ* production in the saturated zone (Fabryka-Martin, 1988). Applications of these assumptions maximize the *in situ* ^{36}Cl production calculations presented in this report.

The total transferred rock-to-ground-water Cl^- concentrations were compared to maximum ambient measured values, and the maximum ^{36}Cl concentrations were adjusted accordingly. For example, for sample SP-1, the maximum total transfer value for Cl^- was 25.40 g/L. However, the maximum average ambient groundwater concentration was 15 mg/L, or 0.059 percent of the estimated total Cl^- transfer concentration. Therefore, the associated maximum ^{36}Cl concentration of 2.52×10^9 atoms/L was reduced by this method to 1.49×10^6 atoms/L to more accurately reflect the possible contribution to ground-water concentrations from *in situ* production. Because of the assumptions discussed earlier, these corrected ^{36}Cl concentrations should be considered as maximum. Additionally, these maximum Cl^- concentrations in ground water would have to be supplied solely by rocks in the aquifer and from no other source.

As previously discussed, the dominant source of neutrons in the deep subsurface (below about 10 m) that are available for activation of stable ^{35}Cl and ^{39}K is the interaction of alpha-emitting progeny from the U and Th decay series and light nuclei. The neutron production rate from this interaction and from the spontaneous fission of naturally occurring ^{238}U can be calculated from the following equation modified from Fabryka-Martin (1988, pages 37-40):

$$Pn = X[U] + Y[Th] + 0.429[U], \quad (10)$$

where

Pn = neutron production rate, in neutrons per gram of rock per year [(n/g)/yr];

X = production of secondary neutrons as a result of α decay of the U series [(n/g)/yr per ppm U];

[U] = U concentration of the rock, in ppm;

Y = production of secondary neutrons as a result of α decay of the Th series [(n/g)/yr per ppm Th];

[Th] = thorium concentration of the rock, in ppm; and

0.429 [U] = neutrons produced by spontaneous fission of ^{238}U [(n/g)/yr per ppm U].

The X and Y factors are determined from the light-element composition of each different rock type in the study area. For example, X for limestone sample SP-1 was determined by dividing the total calculated (n/g)/yr per ppm U by the total weighting factor (table 4). The factor X then was multiplied by the U concentration in ppm to determine the neutron production rate from alpha-particle emissions from the U decay series. The Y factor was calculated in the same manner and multiplied by the Th concentration

to determine the neutron production rate from alpha-particle emissions from the Th decay series. The factor 0.429 [U] in equation (10) accounts for neutrons produced by the spontaneous fission of ^{238}U and includes (1) the atom concentration of a gram of ^{238}U, (2) the spontaneous fission half-life for ^{238}U, (3) the number of neutrons produced per spontaneous fission of ^{238}U, and (4) the fractional concentration of U in the sample in ppm (Fabryka-Martin, 1988, p. 39, 40).

Twenty-five samples of 6 different rock types were analyzed for this study. Table 6 lists the results for each of the samples. The calculated thermal neutron cross sections ranged from 0.0029 cm^2/g of rock in dolomite (SP-4, fig. 1) to 0.0165 cm^2/g of rock in basalt (SP-20, fig. 1). The total neutron production rate for each of the rock types ranged from 0.3 (n/g)/yr in dolomite (SP-4, fig. 1) to 29 (n/g)/yr in rhyolite (SP-17, fig. 1). The total neutron production rates were used in combination with the total reaction cross sections to calculate the *in situ* secular equilibrium $^{36}Cl/Cl$ ratios caused by the two primary reactions that produce ^{36}Cl in the rock matrix at depth. For the reaction $^{35}Cl(n,\gamma)^{36}Cl$, the ratios ranged from 1.4×10^{-15} in basalt (SP-20, fig. 1) to 45×10^{-15} in rhyolite (SP-17, fig. 1). The larger $^{36}Cl/Cl$ ratio for this rhyolite sample is due to the larger U (11.5 ppm) and Th (22.2 ppm) concentration of the rhyolite; for comparison, the U and Th concentrations of this basalt sample were 0.8 and 2.23 ppm, respectively.

For the reaction $^{39}K(n,\alpha)^{36}Cl$, the ratios ranged from less than 0.000001×10^{-15} in limestone (SP-26, fig. 1) to 0.05×10^{-15} in an opal deposit in rhyolite (SP-9, fig. 1). In all samples and rock types in this study, the ^{36}Cl production by neutron activation of stable ^{35}Cl was orders of magnitude greater than production by neutron activation of ^{39}K. Therefore, only the $^{36}Cl/Cl$ ratios and ^{36}Cl concentrations as a result of the reaction $^{35}Cl(n,\gamma)^{36}Cl$, are discussed in the report. Table 6 also lists the calculated equilibrium ^{36}Cl content in the rock matrix. The ^{36}Cl content was smallest in quartzite (SP-24, fig. 1), 0.007×10^5 atoms/cm^3, and was largest in rhyolite and shale (SP-8 and SP-25, fig. 1), 12×10^5 atoms/cm^3.

Table 4 shows an example of the thermal neutron cross section, the total neutron production rate, and the *in situ* secular equilibrium $^{36}Cl/Cl$ ratio calculated for the sedimentary rock sample SP-1, a limestone. The sample was analyzed for the elements shown in table 4, and a sample ppm was calculated using the methods outlined in this report. The weighting factors listed in table 4 were calculated by multiplying the mass stopping power for each element by the corresponding sample ppm expressed as a decimal fraction of the total ppm (J.T. Fabryka-Martin, written commun., 1997). The weight-ed neutron yields were calculated by multiplying the weighting factor by the original calculated neutron yields. The thermal neutron cross section for each of the analyzed elements was calculated by multiplying the sample ppm as a decimal fraction of the total by the absorption cross section in cm^2 and dividing by the atomic weight. The individual thermal neutron cross sections were added to obtain a total thermal neutron cross section.

The X and Y factors were calculated by dividing the total weighted neutron yields by the total weighting factor. The X and Y factors then were multiplied by the corresponding total U and Th sample ppm to arrive at a neutron production rate caused by U and Th decay-series α emissions. In addition, the neutron production rate caused by ^{238}U spontaneous fission was calculated by multiplying the total U sample ppm by the factor of 0.429, as explained in equation (10). The individual neutron production rates were added to obtain a total neutron production rate. To obtain a $^{36}Cl/Cl$ equilibrium ratio, the following equation was modified from (Fabryka-Martin, 1988, p. 208):

$$\frac{^{36}Cl}{Cl} = \frac{(P_n)\times(N)\times(\sigma_{^{35}Cl})}{(\sigma_T)\times(\lambda_{^{36}Cl})}, \qquad (11)$$

where

P_n = total neutron production rate;

N = ^{35}Cl relative isotopic abundance;

$\sigma_{35_{Cl}}$ = thermal neutron absorption cross section of ^{35}Cl;

σ_T = total thermal neutron absoption cross section; and

$\lambda_{36_{Cl}}$ = decay constant for ^{36}Cl.

In this equation, the ^{35}Cl thermal neutron absorption cross section is 4.4×10^{-23} cm^2/atom, the relative isotopic abundance of ^{35}Cl is 0.7577 (Walker and others, 1989), and the ^{36}Cl decay constant is 2.3×10^{-6} yr^{-1}.

The $^{36}Cl/Cl$ ratios estimated for the 25 samples used in this study represent rock types of specific composition as opposed to average composition. Therefore, to obtain values for rock types of average composition, the samples were grouped into the categories of basalt, rhyolite, limestone and dolomite (carbonates), shale, and quartzite (table 7). The U and Th contents were averaged for each category, as were the thermal neutron cross sections, the total neutron production rates, and the *in situ* secular equilibrium $^{36}Cl/Cl$ ratios. The average values are compared in table 7 and figure 3 to average values from Parker's study (1967). The U and Th content, the thermal neutron cross section, and the total neutron production rates for all rock types compare well with the data from Parker's study. Additionally, the histogram in figure 3 shows good correlation between both data sets, further supporting the calculated *in situ* secular equilibrium $^{36}Cl/Cl$ ratios reported for rocks from the eastern Snake River Plain.

Andrews and others (1989) made such calculations for ^{36}Cl production in the Stripa granite using the same methods outlined here for *in situ* production of ^{36}Cl. The Stripa granite is composed of small amounts of neutron-absorbing elements and has a relatively large natural radioelement content. Thus, the neutron flux generated within this granite is among the largest known for crustal rocks (Andrews and others, 1989). The theoretical flux for the Stripa granite was calculated to be 4.07×10^{-4} $(n/cm^2)/s$, whereas the theoretical neutron flux for the surrounding leptite was 0.80×10^{-4} $(n/cm^2)/s$. These values agree to within 15 percent or better of the experimental neutron flux values measured by Andrews and others (1986).

The theoretical flux value was used to calculate neutron-induced production rates of eight isotopes within the Stripa granite, the fracture minerals, and the surrounding leptite. These isotopes were ^{3}He, ^{14}C, ^{36}Cl, ^{129}I, ^{37}Ar, ^{39}Ar, ^{81}Kr, and ^{85}Kr. In calculating the production rates, two assumptions were made. The first assumption was that all the radioisotopes produced within the rock matrix were transferred to the fluids in the rock pore spaces. The second assumption was that the minimum observed porosity for crystalline rocks is 1 percent, an assumption independent of the microdistribution of radionuclide production in relation to the aqueous phase.

The estimated equilibrium number of atoms of ^{36}Cl in 1 cm^3 of the rock matrix was 1.5×10^{6} for the reaction $^{35}Cl(n,\gamma)^{36}Cl$ and 0.04×10^{6} for the $^{39}K(n,\alpha)^{36}Cl$ reaction. For the fracture fluid, the equilibrium number of atoms in 1 cm^3 was 2.5×10^{6} for neutron absorption by ^{35}Cl and was negligible for neutron activation of ^{39}K. For the surrounding leptite rock matrix, the equilibrium number of atoms was 0.19×10^{6} and 0.0067×10^{6} for the two reactions, respectively. As was the case for the rocks from the Snake River Plain aquifer system investigated in this report, the production of ^{36}Cl by activation of ^{39}K in the Stripa granite was insignificant.

The equilibrium $^{36}Cl/Cl$ ratio that resulted from the experimental neutron flux in the rock matrix for the Stripa granite was 215×10^{-15} after 1.5 million years. The equilibrium $^{36}Cl/Cl$ ratio for the surrounding leptite was 41×10^{-15}. Although the $^{36}Cl/Cl$ ratios in the ground water may not reach the same equilibrium ratio as in the aquifer matrix as a result of the smaller residence times, an increase in salinity during transport through the fracture system could result in a Cl^- and $^{36}Cl/Cl$ ratio signature characteristic of the Stripa granite (Andrews and others, 1989). Because of the similarity in

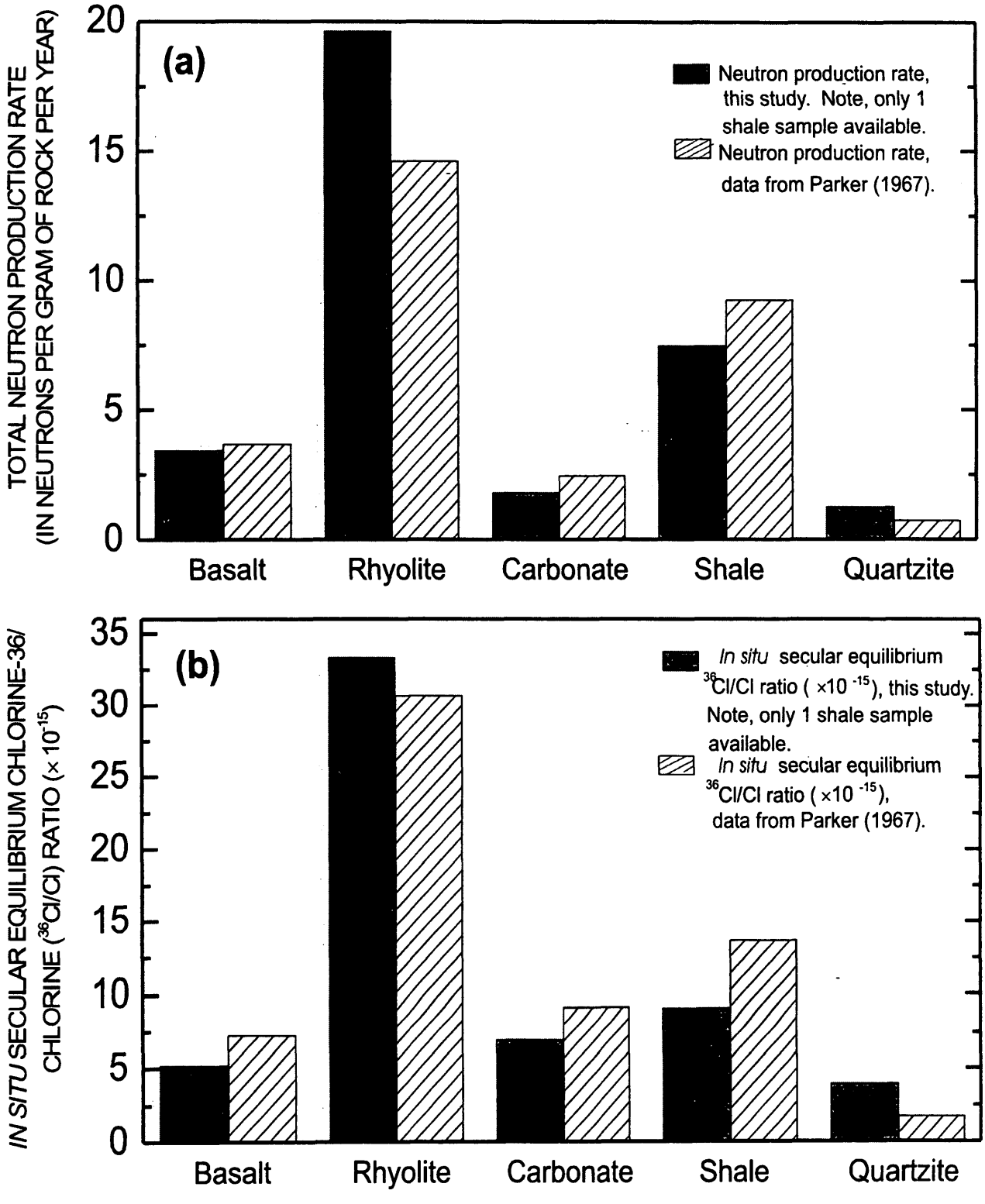

Figure 3. (a) Neutron production rates and (b) *in situ* secular equilibrium chlorine-36/chlorine ratios for rocks of average composition presented in this study and for rocks of average composition from Parker's study (1967).

geochemistry, this $^{36}Cl/Cl$ ratio from the Stripa Granite is comparable to the $^{36}Cl/Cl$ ratio for rhyolite from the eastern Snake River Plain. The estimated equilibrium *in situ* $^{36}Cl/Cl$ ratio for the nine rhyolite samples used in this study ranged from 26×10^{-15} to 45×10^{-15} and the mean was $35\pm5.5\times10^{-15}$ (table 6). The slightly larger $^{36}Cl/Cl$ ratio from the Stripa granite is due to the larger U and Th content of this granite compared to the U and Th content in the average rhyolite from the eastern Snake River Plain; U is 44.1 ppm and Th is 33 ppm in the Stripa granite, and U is 5.96 ppm and Th is 24.1 ppm for average rhyolitic composition from the eastern Snake River Plain (table 7).

If all the Cl^- in the Stripa granite were transferred from the rock to the ground water, a ^{36}Cl concentration of 1.5×10^{11} atoms/L would be produced with an associated fluid chlorinity of 43 g/L. However, the maximum chlorinity present in ground water from the Stripa granite was only 700 mg/L, corresponding to 1.6 percent of the matrix Cl^- transferred to the pore fluids. The resultant corrected ^{36}Cl equilibrium concentration is 2.4×10^{9} atoms/L and is on the same order of magnitude as measured ground-water concentrations in the Stripa granite.

The ^{36}Cl content of Stripa ground water was determined to be a result of *in situ* production because the amount was much larger than what could be derived from cosmogenic or nuclear-fallout sources. Therefore, the input of ^{36}Cl to the ground-water system from cosmogenic and nuclear-fallout sources was determined to be much less significant than the production of ^{36}Cl by neutron capture within the granite. Although this determination ultimately limits the use of ^{36}Cl concentrations for estimation of ground-water residence times in the Stripa granite, Andrews and others (1989) estimated residence time on the rate of ^{36}Cl buildup in the water.

Using the Stripa study as a model, Beasley and others (1993) calculated a theoretical *in situ* produced $^{36}Cl/Cl$ ratio of 1×10^{-18} for the basalt aquifer of the eastern Snake River Plain. This ratio is not measurable by any analytical techniques and *in situ* production was determined to be inconsequential. However, data presented here suggest that the maximum estimated *in situ* $^{36}Cl/Cl$ ratio in basalt rocks of the eastern Snake River Plain ranges from 1.4×10^{-15} to 10×10^{-15} (table 6) or three to four orders of magnitude larger than the theoretical ratio reported by Beasley and others.

This large difference in estimated $^{36}Cl/Cl$ ratios is due to the method of calculation. Beasley and others (1993) estimated the *in situ* contribution for neutron activation of ^{35}Cl dissolved in ground water only. In the present study, possible neutron activation of ^{35}Cl in the aquifer matrix also was considered. Therefore, the ratios calculated in this manner are expected to be orders of magnitude larger as a result of increased neutron production rates and chloride concentrations in the rock compared to those in ground water.

In situ production of ^{36}Cl has been estimated in near-surface environments for a reevaluation of cosmogenic production rates in terrestrial rocks (Phillips and others, 1996). Their evaluation included 17 basalt samples collected from surface exposures on the eastern Snake River Plain. The measured *in situ* $^{36}Cl/Cl$ atom ratios for the 17 samples ranged from $22\pm2\times10^{-15}$ to $249\pm16\times10^{-15}$, and the mean was $125\pm17\times10^{-15}$. For comparison, the estimated *in situ* secular equilibrium $^{36}Cl/Cl$ ratios for the seven basalt samples used in this study ranged from 1.4×10^{-15} to 10×10^{-15}, and the mean was $5.2\pm3.3\times10^{-15}$ (table 6). The 17 basalt samples collected on the Snake River Plain by Phillips and others (1996) were all from surface outcrops. Only one of the seven basalt samples evaluated in this study was an outcrop sample; the remaining six were from depths of 118-728 m below the surface. Therefore, the 17 measured $^{36}Cl/Cl$ atom ratios compare well with the 7 estimated *in situ* ratios, because the surface ratios are expected to be larger by an order of magnitude or more as a result of enhanced surface production of ^{36}Cl by the interaction of cosmic rays with elements in the rocks.

COMPARISON OF *IN SITU* PRODUCED CHLORINE-36 WITH CONCENTRATIONS IN WATER

Chlorine-36 concentrations have been determined for water, snow, and glacial ice samples collected at and near the INEEL (Cecil and others, 1999). In southeastern Idaho and western Wyoming, meteoric concentrations were determined to be less than 1×10^7 atoms/L for recharge, and concentrations between 1×10^7 and 1×10^8 atoms/L were indicative of a nuclear-weapons-tests component from peak ^{36}Cl production in the late 1950s. Chlorine-36 concentrations between 1×10^8 and 1×10^9 atoms/L in ground water and surface water were determined to be representative of resuspension of weapons-test fallout from the landscape, airborne disposal from nuclear-waste processing at the INTEC, or evapotranspiration (ET). Chlorine-36 concentrations larger than 1×10^9 atoms/L were attributable to nuclear-waste disposal practices in the area.

Concentrations of ^{36}Cl in ground-water samples collected downgradient from the INTEC ranged from $10\pm0.2\times10^8$ to $15\pm0.1\times10^{12}$ atoms/L (L.D. Cecil, U.S. Geological Survey, unpub. data, 1999). The associated total Cl^- concentrations ranged from 75 to 220 mg/L. Maximum estimated ^{36}Cl concentrations from *in situ* production for all rock types, corrected to ambient measured Cl^- concentrations, ranged from 2.45×10^5 to 7.68×10^6 atoms/L, or up to seven orders of magnitude smaller than concentrations in ground water near the INTEC (table 8). The ground-water ^{36}Cl concentrations near the INTEC were also three to four orders of magnitude larger than peak weapons-tests fallout for southeastern Idaho and Wyoming (Cecil and others, 1999). Additionally, *in situ* $^{36}Cl/Cl$ ratios for average rock compositions ranged from 4.0×10^{-15} to 33.3×10^{-15} (table 7). For comparison, the range of $^{36}Cl/Cl$ for 254 ground-water samples collected from the Snake River Plain aquifer at and near the INEEL was 31×10^{-15} to 2.9×10^{-9}.

In situ produced ^{36}Cl concentrations compare well with meteoric inputs that may be unaffected by ET. For example, by using calculated fallout rates for ^{36}Cl for precipitation from the study by Cecil and others (1999), a range of possible meteoric concentrations in snow can be calculated. The ^{36}Cl fallout rates determined from separate snowfall events at two different stations in Idaho during 1991 in water equivalent were 0.012 ± 0.002 (atoms/cm^2)/s at Harriman State Park near the Wyoming border and 0.003 ± 0.0015 (atoms/cm^2)/s at Copper Basin in south-central Idaho (fig. 1). Meteoric ^{36}Cl concentrations can be approximated using the ^{36}Cl fallout rate and a range of possible ET rates for the eastern Snake River Plain by using the following equation:

$$\text{meteoric } ^{36}\text{Cl conc.} = \frac{\text{natural } ^{36}\text{Cl fallout rate } \left[\left(\text{atoms/cm}^2\right)/\text{s}\right]}{\left(\text{avg annual precip. (cm/yr)}\right) - \left(\text{avg annual ET (cm/yr)}\right)} \quad (12)$$

where

conc. = concentration

avg = average

precip. = precipitation

ET = evapotranspiration rate

A range of ET rates was used in these calculations in an attempt to account for differences in seasonal distributions of precipitation and ET.

The range of meteoric concentrations using the larger fallout rate for the Harriman site, 0.012 ± 0.002 (atoms/cm^2)/s, and ET rates of 0 and 95 percent, is 6.5×10^6 to 1.3×10^8 atoms/L. Cecil and others (1999) reported a mean ^{36}Cl concentration for 32 surface-water samples collected in southeastern Idaho of 1.5×10^8 atoms/L, which indicates the effects of 95 percent or greater ET. In contrast, ^{36}Cl concentrations for average precipitation for the east coast of the United States, where there is little or no ET, have been determined to be $1.7\pm0.2\times10^6$ at-

oms/L for the period February 1997 through January 1993 (Hainsworth and others, 1994). This average is the same as the calculated ^{36}Cl fallout rate presented here for precipitation not affected by ET in southeastern Idaho. Additionally, meteoric ^{36}Cl ground-water concentrations from the eastern Snake River Plain aquifer range from 1.0×10^{5} to 5.0×10^{6} atoms/L, which supports the idea that no significant ^{36}Cl is being picked up in the shallow subsurface by rapidly infiltrating recharge that would not be significantly affected by ET. These meteoric concentrations are in contrast to the average ^{36}Cl concentration in the 32 surface-water samples, 1.5×10^{8} atoms/L, that would be expected to be influenced by ET processes.

For comparison to measured ^{36}Cl concentrations in surface water, an average concentration of ^{36}Cl produced in surface water was estimated. Turekian (1969) compiled the average composition of surface water for nearly all the elements, and these data were used to calculate an average *in situ* produced concentration for ^{36}Cl. An average *in situ* equilibrium ^{36}Cl concentration for surface water of 1.83×10^{4} atoms/L was calculated. Although this relatively small ^{36}Cl concentration calculated in this manner is a first-order approximation, it suggests that the *in situ* contribution from surface water of average composition is insignificant compared to the contributions from weapons-tests fallout, natural atmospheric production, overland runoff containing near-surface-produced ^{36}Cl, and concentrations as a result of nuclear-waste disposal at the INEEL.

Two snow samples were collected at the INEEL (INEEL #1 and INEEL #2, fig. 1) during nuclear-waste reprocessing operations, and resultant ^{36}Cl fallout rates were determined for comparison to possible meteoric concentrations. The largest fallout rate, 12±2.4 (atoms/cm^2/)s for INEEL #2, was used to calculate a contribution of ^{36}Cl to the Earth's surface from the INTEC. Again, by application of equation (12), the possible contribution to ground-water concentrations from precipitation affected by waste-processing operations at the INEEL ranged from 1.7×10^{10} atoms/L for no ET to 3.8×10^{11} atoms/L for 95-percent ET. These concentrations are four to five orders of magnitude larger than estimated natural meteoric contributions to ground water ^{36}Cl concentrations in the eastern Snake River Plain aquifer. Considering groundwater residence time and rapid infiltration of recharge in the eastern Snake River Plain aquifer, it is highly unlikely that significant ^{36}Cl concentrations from *in situ* production occur.

SUMMARY

Twenty-five whole-rock samples were collected from basalt, rhyolite, limestone, dolomite, shale, and quartzite rock types in the eastern Snake River Plain aquifer. *In situ* production of ^{36}Cl in the rock samples resulting from nuclear interactions between stable nuclides and particles given off during the radioactive transformation of U and Th decay-series isotopes was determined. Calculated ratios of $^{36}Cl/Cl$ in these rocks, as a result of neutron activation of stable chlorine-35, ranged from 1.4×10^{-15} for basalt to 45×10^{-15} for rhyolite. The associated neutron production rates calculated for these rock types were 2.5 (n/g)/yr for the basalt and 29 (n/g)/yr for the rhyolite. The larger neutron production rate for this rhyolite sample is due to the larger U (11.5 ppm) and Th (22.2 ppm) concentration of the rhyolite; for comparison, the U and Th concentrations of this basalt sample 0.8 and 2.23 ppm, respectively.

Corrected concentrations of ^{36}Cl in ground water were estimated by taking into account Cl^- concentration, rock porosity, and the calculated $^{36}Cl/Cl$ ratios. In basalt and rhyolite, the maximum ^{36}Cl concentrations were 1.77×10^{6} and 7.68×10^{6} atoms/L, respectively. These maximum estimated ^{36}Cl concentrations in ground water from *in situ* production are on the same order of magnitude as natural concentrations in meteoric water. In contrast, the ^{36}Cl concentration measured in ground water collected near the INTEC was reported to be $15\pm0.1\times10^{12}$ atoms/L, or up to seven orders of magnitude larger than *in situ* or meteoric concentrations. *In situ* $^{36}Cl/Cl$

ratios in ground water from rock with average compositions from this study ranged from 4.0×10^{-15} to 33.3×10^{-15}. For comparison, the range of $^{36}Cl/Cl$ for 254 ground-water samples collected from the Snake River Plain aquifer at and near the INEEL was 31×10^{-15} to 2.9×10^{-9}. Based on these results, *in situ* production of ^{36}Cl is insignificant compared to concentrations measured in ground water near buried and injected nuclear waste at the INEEL.

REFERENCES CITED

Ackerman, D.J., 1991, Transmissivity of the Snake River Plain aquifer at the Idaho National Engineering Laboratory, Idaho: U.S. Geological Survey Water-Resources Investigations Report 91-4058 (DOE/ID-22097), 35 p.

Anders, E., and Ebihara, M., 1982, Solar system abundance of the elements: Geochemica et Cosmochemica Acta, v. 46, p. 2363-2380.

Andrews, J.N., Davis, S.N., Fabryka-Martin, J., Fontes, J-Ch., Lehmann, B.E., Loosli, H.H., Michelot, J-L., Moser, H., Smith, B., and Wolf, M., 1989, The *in situ* production of radioisotopes in rock matrices with particular reference to the Stripa granite: Geochemica et Cosmochemica Acta, v. 53, p. 1803-1815.

Andrews, J.N., and Fontes, J-Ch., 1992, Importance of the *in situ* production of ^{36}Cl, ^{36}Ar, and ^{14}C in hydrology and hydrogeochemistry: International Atomic Energy Agency, IAES-SM-319/12, p. 245-269.

Andrews, J.N., Fontes, J-Ch., Michelot J-L., and Elmore, D., 1986, *In situ* ^{36}Cl production and groundwater evolution in crystalline rocks at Stripa, Sweden: Earth and Planetary Science Letters, 77, p. 49-58.

Aruscavage, P., 1990, Determination of Cl^- in geologic materials by ion-selective electrode following $KMnO_4$-H_2SO_4-HF dissolution, *in* Arbogast, B.F., ed., Quality Assurance Manual for the Branch of Geochemistry: U.S. Geological Survey Open-File Report 90-668, p. 119-122.

Baedecker, P.A., and McKown, D.M., 1987, Instrumental neutron activation analysis of geochemical samples, *in* Baedecker, P.A., ed., Methods for Geochemical Analysis: U.S. Geological Survey Bulletin 1770, p. H1-H14.

Beasley, T.M., Cecil, L.D., Sharma, P., Kubik, P.W., Fehn, U., Mann, L.J., and Gove, H.E., 1993, Chlorine-36 in the Snake River Plain aquifer at the Idaho National Engineering Laboratory-Origin and Implications: Ground Water, v. 31, no. 2, p. 302-310.

Cecil, L.D., Beasley, T.M., Pittman, J.R., Michel, R.L., Kubik, P.W., Sharma, P., Fehn, U., and Gove, H.E., 1992, Water infiltration rates in the unsaturated zone at the Idaho National Engineering Laboratory from chlorine-36 and tritium profiles, and neutron logging, *in* Kharaka, Y.F., and Maest, A.S., eds., Water-Rock Interactions, v. 1: Rotterdam, A.A. Balkema p. 709-714.

Cecil, L.D., Green, J.R., Vogt, S., Frape, S.K., Davis, S.N., Cottrell, G.L., and Sharma, P., 1999, Chlorine-36 in water, snow, and mid-latitude glacial ice of North America: Meteoric and weapons-tests production in the vicinity of the Idaho National Engineering and Environmental Laboratory, Idaho: U.S. Geological Survey Water-Resources Investigations Report 99-4037 (DOE/ID-22156), 27 p.

Cecil, L.D., Green, J.R., Vogt, S., Michel, R.L., and Cottrell, G., 1998, Isotopic composition of ice cores and meltwater from Upper Fremont Glacier and Galena Creek Rock Glacier, Wyoming: Geographiska Annaler, v. 80A, p. 287-292.

Cecil, L.D., and Vogt, S., 1997, Identification of bomb-produced chlorine-36 in mid-latitude glacial ice of North America: Nuclear Instruments and Methods in Physics Research B123, p. 287-289.

Cecil, L.D., Welhan, J.A., Green, J.R., Frape, S.K., and Sudizky, E.R., in press. Use of chlorine-36 to determine regional-scale aquifer dispersivity, eastern Snake River Plain aquifer, Idaho/USA. Nuclear Instruments and Methods in Physics Research B: Holland, Elsevier Science, 9 p.

Clawson, K.L., Start, G.E., and Ricks, N.R., eds., 1989, Climatography of the Idaho National Engineering Laboratory: U.S. Department of Commerce, National Oceanic and Atmospheric Administration, DOE/ID-12118, 155 p.

Davis, S.N., Cecil, L.D., Zareda, M., and Sharma, P., 1998, Chlorine-36 and the initial value problem: Hydrogeology Journal, v. 6, no. 1, p. 104-113.

Dobrin, M.B., 1976, Introduction to geophysical prospecting: McGraw-Hill, Inc., 459 p.

Fabryka-Martin, J.T., 1988, Production of radionuclides in the earth and their hydrogeologic significance with emphasis on chlorine-36 and iodine-129: University of Arizona, Ph.D. dissertation, 400 p.

Faure, Gunter, 1986, Principles of isotope geology: New York, John Wiley and Sons, 589 p.

Freeze, R.A., and Cherry, J.A., 1979, Groundwater: Prentice-Hall, 604 p.

Garabedian, S.P., 1992, Hydrology and digital simulation of the regional aquifer system, eastern Snake River Plain, Idaho: U.S. Geological Survey Professional Paper 1408-F, 102 p.

Gifford, S.K., Bentley, H., and Graham, D.L., 1985, Chlorine isotopes as environmental tracers in Columbia River basalt groundwaters: Memoirs, Hydrogeology of Rocks of Low Permeability, International Association of Hydrogeologists, Tucson, AZ, v. XVII, part 1, p. 417-429.

Hainsworth, L.J., Mignerey, A.C., Helz, G.R., Sharma, P., and Kubik, P.W., 1994, Modern chlorine-36 deposition in southern Maryland, U.S.A., *in* Nuclear Instruments and Methods in Physics Research B92: Holland, Elsevier Science, p. 345-349.

Knobel, L.L., Cecil, L.D., and Woods, T., 1995, Chemical composition of selected core samples, Idaho National Engineering Laboratory, Idaho: U.S. Geological Survey Open-File Report 95-748, 59 p.

Kuntz, M.A., Champion, D.E., Lefevzre, R.F., and Covington, H.R., 1988, Geologic map of the Craters of the Moon, Kings Bowl, and Wapi Lava Fields in the Great Rift Volcanic Rift Zone, south-central Idaho: U.S. Geological Survey Miscellaneous Investigations Series Map, I-1632, scale 1:1,000,000.

Lichte, R.E., Golightly, D.W., and LaMothe, P.J., 1987, Inductively coupled plasma atomic emission spectrometry, *in* Baedecker, P.A., ed., Methods for Geochemical Analysis: U.S. Geological Survey Bulletin 1770, p. B1-B10.

Nace, R.L., Voegeli, P.T., Jones, J.R., and Deutsch, Morris, 1975, Generalized geologic framework of the National Reactor Testing Station, Idaho: U.S. Geological Survey Professional Paper 725-B, 49 p.

Parker, R.L., 1967, Composition of the Earth's crust: U.S. Geological Survey Professional Paper 440-D, 19 p.

Phillips, F.M., Zreda, M.G., Flinsch, M.R., Elmore, D., and Sharma, P., 1996, A reevaluation of cosmogenic ^{36}Cl production rates in terrestrial rocks: Geophysical Research Letters, v. 23 (9), p. 949-952.

Schaeffer, O.A., Thompson, S.O., and Lark, N.L, 1960, Chlorine-36 radioactivity in rain: Journal of Geophysical Research, v. 65, p. 4013-4016.

Turekian, K.K., 1969, The oceans, streams, and atmosphere, *in* Wedepohl, K.H., ed., Handbook of Geochemistry, v. 1: New York, Springer-Verlag p. 297-323.

Walker, W.W., Parrington, J.R., and Feiner, F., 1989, Nuclides and isotopes, chart of the nuclides, 14th ed.: San Jose, Calif., General Electric Co., 57 p.

Whitehead, R.L., 1992, Geohydrologic framework of the Snake River Plain regional aquifer system, Idaho and eastern Oregon: U.S. Geological Survey Professional Paper 1408-B, 32 p.

DEFINITIONS FOR CHEMICAL SYMBOLS AND NOTATIONS USED IN TABLES 1, 2, 3, and 4

Al	Aluminum
B	Boron
Be	Beryllium
cm^2/g	Square centimeters per gram
C	Carbon
Ca	Calcium
Cl	Chlorine
F	Fluorine
Fe	Iron
Gram atomic weight	Weighted average mass of all isotopes of an element relative to the mass of pure carbon-12
Gd	Gadolinium
H,w	Hydrogen from water
ICP-AES	Inductively coupled plasma-atomic emission spectrometry
ISEP	Ion-selective electrode potentiometry
INAA	Instrumental neutron activation analysis
K	Potassium
Li	Lithium
LOI	Loss on ignition
Mg	Magnesium
Mn	Manganese
(n/g)/yr	Neutrons per gram of rock per year
Na	Sodium
O,r	Oxygen as structural component of rock matrix
O,w	Oxygen from water
P	Phosphorus
ppm	Parts per million by weight
Si	Silicon
Sm	Samarium
Tb	Terbium
Th	Thorium
Ti	Titanium
Total (adj.)	Sum of all elements including H,w and O,w from water adjusted to equal 1,000,000 ppm
Total (raw)	Sum of all elements except H,w and O,w from water adjusted to equal 1,000,000 ppm
U	Uranium
Z	Atomic number

Table 1. Data for calculating thermal cross sections for neutron absorption, igneous rock samples from the eastern Snake River Plain aquifer.

[Sample locations are shown on figure 1. Source of data: major rock-forming elements as oxides in weight percent, trace elements in ppm by weight, and volatile components in weight percent are from the Idaho State University Department of Geology Geochemistry Laboratory and were determined by ICP-AES, INAA, or LOI (value in parentheses indicates that the element's concentration was outside the calibration range of the instrument during analysis and that the value was reduced to make the laboratory weight-percent data equal 100 percent); unmarked chlorine values in weight percent are from the U.S. Geological Survey Branch of Geochemistry Laboratory and were determined by ISEP; values marked with an asterisk (*) are from Parker [directly for basalt samples and from geochemical equivalent for rhyolite samples (felsic granite)] (1967, table 19, p. D13-D14). Calculations: Gd values were calculated using chondritic trace-element ratios; carbon values marked with @ symbol were calculated under the assumption that the moles of carbon were equivalent to the sum of the moles of calcium and magnesium; values for H,w and O,w were calculated under the assumption that the difference between the raw and adj. totals plus excess LOI values was attributable to water content (both water of hydration and pore water); the value for O,r was calculated from oxide weight-percent data. For a detailed explanation of calculations and conversions, see section of text, "Data Processing." Symbol: <, less than]

			Sample identifier and rock type					
Z (Atomic number)	Element	Gram atomic weight	SP-5 ppm rhyolite outcrop	SP-6 ppm rhyolite outcrop	SP-7 ppm rhyolite outcrop	SP-8 ppm rhyolite Depth, 10 meters	SP-9 ppm opal in rhyolite Depth, 10 meters	SP-10 ppm rhyolite outcrop
14	Si	28.1	343,302	345,718	314,633	353,104	345,625	338,660
13	Al	27.0	56,153	64,410	58,588	60,864	64,780	64,304
26	Fe	55.8	10,649	13,137	12,670	10,338	2,254	14,458
20	Ca	40.1	15,223	5,503	36,664	3,859	1,572	4,431
12	Mg	24.3	5,549	724	603	422	121	603
11	Na	23.0	25,223	26633	26,262	25,965	964	27,820
19	K	39.1	38,935	44,746	43,500	44,580	7,222	44,497
15	P	30.97	175	218	131	131	175	175
3	Li	6.9	*40	*40	*40	*40	*15	*40
4	Be	9.01	*5.5	*5.5	*5.5	*5.5	*.5	*5.5
5	B	10.8	*15	*15	*15	*15	*35	*15
6	C	12.0	*300	*300	*300	*300	@531	*300
9	F	19	*800	*800	*800	*800	*270	*800
1	H,w	1.0	3,506.37	2,018.39	6,242.28	1,944.54	13,180.93	3,630.32
22	Ti	47.9	719	1,079	959	899	1439	1,499
25	Mn	54.9	77	1,007	232	310	<77	232
62	Sm	150.4	17.3	15.7	11.1	13.6	4.28	12.9
65	Tb	158.9	2.28	2.2	1.33	1.94	.43	1.89
64	Gd	157.3	15.37	14.53	9.26	12.74	3.17	12.30
8	O,r	16.0	471,195	477,325	448,158	480,228	457,162	469,421
8	O,w	16.0	27,828.18	16,018.88	49,541.63	15,432.78	104,610.09	28,811.89
92	U	238.0	4.9	4.4	5.1	6.2	5.3	5.3
90	Th	232.0	25.1	25.4	28.8	27.7	20.3	24.9
17	Cl	35.5	*240	*240	600	700	*10	*240
	Total (raw)		968,665.45	981,962.73	944,216.09	982,622.68	882,208.98	967,557.79
	Total (adj.)		1,000,000	1,000,000	1,000,000	1,000,000	1,000,000	1,000,000

Table 1. Data for calculating thermal cross sections for neutron absorption, igneous rock samples from the eastern Snake River Plain aquifer—Continued

Z (Atomic number)	Element	Gram atomic weight	Sample identifier and rock type: SP-13 ppm rhyolite outcrop	SP-15 ppm basalt Depth, 728 meters	SP-16 ppm basalt Depth, 158 meters	SP-17 ppm rhyolite Depth, 136 Meters	SP-18 ppm basalt Depth, 180 meters	SP-19 ppm basalt Depth, 118 meters
14	Si	28.1	346,419	210,348	212,685	(353,337)	222,969	215,490
13	Al	27.0	62,081	69,861	77,800	66,156	85,739	83,622
26	Fe	55.8	8,550	90,945	85,504	12,903	81,618	97,164
20	Ca	40.1	11,078	77,545	73,614	5,003	79,332	76,259
12	Mg	24.3	784	33,291	49,575	1,025	50,359	46,982
11	Na	23.0	25,594	15,727	17,582	31,974	18,250	18,695
19	K	39.1	44,165	12,369	3,653	38,187	3,736	4,400
15	P	30.97	175	3,710	1,091	87	1,397	1,920
3	Li	6.9	*40	*15	*15	*40	*15	*15
4	Be	9.01	*5.5	*.4	*.4	*5.5	*.4	*.4
5	B	10.8	*15	*5	*5	*15	*5	*5
6	C	12.0	*300	*100	*100	*300	*100	*100
9	F	19	*800	*370	*370	*800	*370	*370
1	H,w	1.0	2,579.75	7,065.57	5,863.45	103.33	1,034.88	1,375.94
22	Ti	47.9	480	16,247	10,491	959	10,611	13,069
25	Mn	54.9	310	1,471	1,317	387	1,317	1,394
62	Sm	150.4	9.91	7.51	4.75	15.44	4.8	5.68
65	Tb	158.9	1.57	.94	.05	4.31	.6	.75
64	Gd	157.3	9.96	6.45	3.87	22.63	4.12	5.05
8	O,r	16.0	475,864	404,786	413,688	487,582	434,872	428,105
8	O,w	16.0	20,474.11	56,075.49	46,534.97	820.09	8,213.29	10,920.08
92	U	238.0	5.1	1.1	.8	11.5	.6	.5
90	Th	232.0	19.1	2.54	1.71	22.2	1.31	1.6
17	Cl	35.5	*240	*50	100	*240	*50	100
	Total (raw)		976,946.14	936,858.94	947,601.58	999,076.58	990,751.83	987,703.98
	Total (adj.)		1,000,000	1,000,000	1,000,000	1,000,000	1,000,000	1,000,000

Table 1. Data for calculating thermal cross sections for neutron absorption, igneous rock samples from the eastern Snake River Plain aquifer—Continued

Z (Atomic number)	Element	Gram atomic weight	Sample identifier and rock type			
			SP-20 ppm basalt Depth, 193 meters	SP-21 ppm basalt Depth, 259 meters	SP-22 ppm basalt outcrop	SP-23 ppm rhyolite outcrop
14	Si	28.1	209,880	214,555	227,176	347,775
13	Al	27.0	79,388	70,390	75,683	60,864
26	Fe	55.8	98,719	94,055	66,071	15,002
20	Ca	40.1	70,970	57,176	66,610	3,431
12	Mg	24.3	43,665	30,035	45,293	543
11	Na	23.0	18,917	23,294	17,211	26,707
19	K	39.1	5,230	14,611	26,980	41,840
15	P	30.97	2,662	1,353	2,269	131
3	Li	6.9	*15	*15	*15	*40
4	Be	9.01	*.4	*.4	*.4	*5.5
5	B	10.8	*5	*5	*5	*15
6	C	12.0	*100	*100	*100	*300
9	F	19	*370	*370	*370	*800
1	H,w	1.0	3,882.04	8,489.93	5,241.73	2,813.21
22	Ti	47.9	16,247	15,887	4,736	1,259
25	Mn	54.9	1,471	1,549	1,162	465
62	Sm	150.4	7.39	13.77	5.07	14.25
65	Tb	158.9	.96	2.22	.73	2.2
64	Gd	157.3	6.50	13.99	4.78	14.07
8	O,r	16.0	417,451	400,495	419,409	475,383
8	O,w	16.0	30,809.68	67,380.12	41,600.81	22,326.97
92	U	238.0	.8	3.0	1.2	5.8
90	Th	232.0	2.23	6.57	5.28	23.0
17	Cl	35.5	200	200	*50	*240
	Total (raw)		965,308.28	924,129.95	953,157.46	974,859.82
	Total (adj.)		1,000,000	1,000,000	1,000,000	1,000,000

Table 2. Data for calculating thermal cross sections for neutron absorption, sedimentary rock samples from the eastern Snake River Plain aquifer.

[Sample locations are shown on figure 1. Source of data: major rock-forming elements as oxides in weight percent, trace elements in ppm by weight, and volatile components in weight percent are from the Idaho State University Department of Geology Geochemistry Laboratory and were determined by ICP-AES, INAA, or LOI; unmarked chlorine values in weight percent are from the U.S. Geological Survey Branch of Geochemistry Laboratory and were determined by ISEP; values marked with an asterisk (*) are from Parker (1967, table 19, p. D13-D14). Calculations: Gd values were calculated using chondritic trace-element ratios; carbon was calculated under the assumption that LOI values resulted from volatilization of carbonate; values for H,w and O,w were calculated under the assumption that the difference between the raw and adj. totals plus excess LOI values was attributable to water content; the value for O,r was calculated from oxide weight-percent and LOI data. For a detailed explanation of calculations and conversions, see section of text, "Data Processing." Symbols: -bd-, below detection limit; <, less than]

			Sample identifier and rock type						
Z (Atomic number)	Element	Gram atomic weight	SP-1 ppm limestone outcrop	SP-2 ppm limestone Depth, 10 meters	SP-3 ppm limestone outcrop	SP-4 ppm dolomite outcrop	SP-12 ppm limestone outcrop	SP-25 ppm shale outcrop	SP-26 ppm limestone outcrop
14	Si	28.1	7,947	10,564	8,554	3,085	19,960	226,241	-bd-
13	Al	27.0	1,376	2,064	1,217	1,429	1,747	62,452	-bd-
26	Fe	55.8	233	544	233	1,166	777	30,704	311
20	Ca	40.1	382,508	381,865	383,586	217,555	369,572	63,394	385,939
12	Mg	24.3	4,522	2,714	3,317	120,681	3,076	38,659	2,835
11	Na	23.0	74	148	74	223	74	6,825	148
19	K	39.1	415	830	249	747	913	26,731	0
15	P	30.97	87	131	44	44	218	1,222	262
3	Li	6.9	*5	*5	*5	*5	*5	*60	*5
4	Be	9.01	*.5	*.5	*.5	*.5	*.5	*3	*.5
5	B	10.8	*20	*20	*20	*20	*20	*100	*20
6	C	12.0	118,201	117,164	117,519	128,108	116,318	*10,000	115,718
9	F	19	*330	*330	*330	*330	*330	*500	*330
1	H,w	1.0	340.37	284.27	569.56	1,459.63	250.74	12,664.38	3,243.86
22	Ti	47.9	<60	60	<60	<60	60	3,477	240
25	Mn	54.9	<77	<77	<77	155	<77	1,704	155
62	Sm	150.4	.39	.69	.72	.12	.64	4.53	.72
65	Tb	158.9	.05	.09	.11	.01	.07	.66	.06
64	Gd	157.3	.34	.61	.71	.08	.50	4.30	.47
8	O,r	16.0	481,137	480,816	479,607	513,007	484,485	411,732	464,892
8	O,w	16.0	2,701.35	2,256.13	4,520.32	11,584.32	1,990.03	100,510.46	25,744.81
92	U	238.0	1.9	2.5	2.9	.2	2.3	2.6	4.3
90	Th	232.0	.1	.21	.18	.14	.22	9.07	.28
17	Cl	35.5	100	200	*150	400	200	*3,000	*150
	Total (raw)		996,958.28	997,459.60	994,910.12	986,956.05	997,759.23	886,825.16	971,011.33
	Total (adj.)		1,000,000	1,000,000	1,000,000	1,000,000	1,000,000	1,000,000	1,000,000

Table 3. Data for calculating thermal cross sections for neutron absorption, metamorphic rock samples from the eastern Snake River Plain aquifer.

[Sample locations are shown on figure 1. Source of data: major rock-forming elements as oxides in weight percent, trace elements in ppm by weight, and volatile components in weight percent are from the Idaho State University (ISU) Department of Geology Geochemistry Laboratory and were determined by ICP-AES, INAA, or LOI (value in parentheses indicates that the element's concentration was outside the calibration range of the instrument during analysis and that the value was reduced to make the laboratory weight-percent data equal 100 percent); unmarked chlorine values in weight percent are from the U.S. Geological Survey Branch of Geochemistry Laboratory and were determined by ISEP; values marked with an asterisk (*) are from Parker [directly for basalt samples and from geochemical equivalent for quartzite (sandstone)] (1967, table 19, p. D13-D14). Assumption: LOI values provided by the ISU Laboratory were assumed to result from volatilization of carbonate or water. Calculations: Gd values were calculated using chondritic trace-element ratios; carbon values marked with @ symbol were calculated under the assumption that the moles of carbon were equivalent to the sum of the moles of calcium and magnesium; values for H,w and O,w were calculated under the assumption that the difference between the raw and adj. totals plus the excess LOI values was attributable to water content (both the water of hydration and pore water); the value for O,r was calculated from oxide weight percent and LOI data. For a detailed explanation of calculations and conversions, see section of text, "Data Processing." Symbols: - bd-, below detection limit; <, less than]

			Sample identifier and rock type	
Z (Atomic number)	Element	Gram atomic weight	SP-11 ppm quartzite outcrop	SP-24 ppm quartzite outcrop
14	Si	28.1	342,353	(463,513)
13	Al	27.0	16,883	-bd-
26	Fe	55.8	5,441	155
20	Ca	40.1	69,969	0
12	Mg	24.3	5,126	181
11	Na	23.0	371	148
19	K	39.1	8,966	2,657
15	P	30.97	524	131
3	Li	6.9	*15	*15
4	Be	9.01	*.5	*.5
5	B	10.8	*35	*35
6	C	12.0	@23,501	@89
9	F	19	*270	*270
1	H,w	1.0	2,379.16	295.54
22	Ti	47.9	719	420
25	Mn	54.9	620	155
62	Sm	150.4	2.01	.28
65	Tb	158.9	.27	.04
64	Gd	157.3	1.81	.26
8	O,r	16.0	503,836	529,578
8	O,w	16.0	18,882.17	2,345.53
92	U	238.0	1.4	.3
90	Th	232.0	3.68	.55
17	Cl	35.5	100	*10
		Total (raw) =	978,738.67	997,358.93
		Total (adj.) =	1,000,000	1,000,000

Table 4. Example of calculated thermal neutron cross section for neutron absorption, total neutron production rate, and *in situ* secular equlibrium chlorine-36/chlorine (^{36}Cl/Cl) ratio for sedimentary rock sample SP-1, limestone, eastern Snake River Plain aquifer.

[Sample locations are shown on figure 1. See text for explanation of mass stopping power, weighting factor, X and Y factors, weighted neutron yields, and thermal cross sections. Mass stopping power, neutron yields, and absorption cross sections from Fabryka-Martin (1988). Mass stopping power is given for each element for an alpha particle of energy 8.0 million electron volts (MeV). Mass stopping power units: MeV per gram of rock per square centimeter. Sample ppm from table 2; <, less than]

		Neutron yield				Weighted neutron yield	
Element	Mass stopping power	(n/g)/yr rock per ppm U	(n/g)/yr rock per ppm Th	Sample ppm	Weighting factor	(n/g)/yr rock per ppm U	(n/g)/yr rock per ppm Th
Si	454	0.69	0.339	7.947	3.61	2.49	1.22
Al	444	5.116	2.585	1,376	.61	3.13	1.58
Fe	351	.187	.208	233	.08	.02	.02
Ca	428	.282	.026	382,508	163.71	46.17	4.26
Mg	461	5.834	2.564	4,522	2.08	12.16	5.35
Na	456	12.535	5.959	74	.03	.42	.20
K	414	.89	.08	415	.17	.15	.01
P	433	4.473	.573	87	.04	.17	.02
Li	548	23.86	10.54	5	.003	.07	.03
Be	529	265.948	91.561	.5	.0003	.07	.02
B	527	62.551	19.779	20	.01	.66	.21
C	561	.456	.179	118,201	66.31	30.24	11.87
F	472	41.33	16.362	330	.16	6.44	2.55
O	527	.236	.084	483,838.35	254.98	60.18	21.42
			Total	999,556.85	491.8	162.35	48.76

Element	Gram atomic weight	Sample ppm	Neutron absorption cross section (barns/atom)	Thermal neutron cross section (cm^2/g)
Si	28.1	7,947	0.17	0.000029
Al	27.0	1,376	.233	.000007
Fe	55.8	233	2.56	.000006
Ca	40.1	382,508	.43	.002469
Mg	24.3	4,522	.063	.000007
Na	23.0	74	.53	.000001
K	39.1	415	2.1	.000013
P	30.97	87	.18	< .000001
Li	6.9	5	71	.000031
Be	9.01	.5	.0092	< .000001
B	10.8	20	764	.000852
C	12.0	118,201	.0035	.000021
F	19.0	330	.0096	< .000001
H	1.0	340.37	.33	.000068
Ti	47.9	60	6.1	.000005
Mn	54.9	77	13.3	.000011
Sm	150.4	.39	5,600	.000009
Gd	157.3	.34	49,000	.000064
O	16.0	483,838.35	.00028	.000005
	Total	1,000,034.95		.0036

		Neutron production rate [(n/g)/yr]
(X factor = .330)	(Total U ppm = 1.9) =	0.63
(Y factor = .099)	(Total Th ppm = .1) =	.0099
	^{238}U spontaneous fission =	.815
	Total neutron production rate[(n/g)/yr)] =	1.5

Calculated *in situ* secular equilibrium ^{36}Cl/Cl ratio ($\times 10^{-15}$) = 5.9

Table 5. Measured and estimated gadolinium concentrations for 56 basalt samples from the eastern Snake River Plain aquifer.

[Measured gadolinium concentrations taken from Knobel and others (1995). Estimated gadolinium concentrations calculated with equations 2-5 in text. ppm, parts per million by weight]

Measured gadolinium (ppm)	Estimated gadolinium (ppm)	Measured gadolinium (ppm)	Estimated gadolinium (ppm)
11	10	8.1	7.8
11	10	7.8	7.7
9.8	9.2	7.6	7.6
9.2	9	7.7	7.1
9.8	9.2	7.3	7.4
9.2	9.1	7.8	7.6
8.4	7.9	7.6	7.1
7.6	6.8	14	13
9.6	7.3	10	9.7
7.6	8.4	9.6	9.1
7.4	7.1	9.9	9.3
7.2	7.0	11	9.7
6.6	6.8	9.2	9.1
6.7	6.3	7.6	7.2
4.6	5.5	7.1	7.0
5.8	4.7	5.6	5.3
7.4	6.2	6.6	6.3
7	7.0	5.5	5.3
8	7.0	6.9	6.5
7.2	7.5	7.2	6.5
6.3	6.6	7.6	7.1
6.6	6.1	6.9	6.4
6.1	6.2	6.4	6
6.7	6.3	6.6	6.3
7	6.4	6.5	6.3
6.4	6.7	6.6	6.4
8.9	7.1	3.8	3.7
7.8	8.1	3.9	3.8

Measured mean and associated uncertainty, 7.7 ± 1.8 ppm.
Estimated mean and associated uncertainty, 7.3 ± 1.7 ppm.

Table 6. Calculated thermal neutron cross sections for neutron absorption, total neutron production rate, *in situ* secular equilibrium chlorine-36/chlorine ($^{36}Cl/Cl$) ratios, and equilibrium chlorine-36 concentration in the rock matrix, eastern Snake River Plain aquifer.

[Sample locations are shown on figure 1; cm^2/g, square centimeters per gram; Cl, chlorine; cm^3, cubic centimeters; K, potassium; <, less than]

Sample identifier and rock type	Thermal neutron cross section (cm^2/g)	Total neutron production rate (neutrons/ gram of rock/year)	*In situ* secular equilibrium $^{36}Cl/Cl$ ratio due to $^{35}Cl(n,\gamma)^{36}Cl$ ($\times 10^{-15}$)	*In situ* secular equilibrium $^{36}Cl/Cl$ ratio due to $^{39}K(n,\alpha)^{36}Cl$ ($\times 10^{-15}$)	Equilibrium ^{36}Cl in rock matrix ($\times 10^5$ atoms/cm^3)
Igneous					
SP-5, rhyolite	0.0085	19	32	0.02	3.3
SP-6, rhyolite	.0084	19	32	.02	3.3
SP-7, rhyolite	.0080	20	37	.009	9.4
SP-8, rhyolite	.0078	22	41	.008	12
SP-9, opal deposit in rhyolite	.0069	13	26	.05	.11
SP-10, rhyolite	.0082	20	35	.02	3.6
SP-13, rhyolite	.0072	16	33	.02	3.3
SP-15, basalt	.0094	2.9	4.5	.005	.10
SP-16, basalt	.0077	2.3	4.2	.0005	.19
SP-17, rhyolite	.0093	29	45	.03	4.8
SP-18, basalt	.0069	1.8	3.7	.0007	.08
SP-19, basalt	.0077	1.7	3.3	.0004	.15
SP-20, basalt	.0165	2.5	1.4	.0008	.13
SP-21, basalt	.0113	8.2	10	.005	.92
SP-22, basalt	.0076	4.7	9.1	.01	.20
SP-23, rhyolite	.0083	19	34	.02	3.6
Sedimentary					
SP-1, limestone	.0036	1.5	5.9	.00002	.25
SP-2, limestone	.0037	1.9	7.5	.00002	.65
SP-3, limestone	.0037	2.2	8.6	.00001	.55
SP-4, dolomite	.0029	.3	1.6	.000001	.28
SP-12, limestone	.0037	1.8	7.1	.00002	.61
SP-25, shale	.0120	7.5	9.1	.0006	12
SP-26, limestone	.0042	3.2	11	<.000001	.72
Metamorphic					
SP-11, quartzite	.0048	2.1	6.4	.007	.30
SP-24, quartzite	.0035	.4	1.5	.0003	.007

Table 7. Calculated thermal neutron cross sections for neutron absorption, total neutron production rates, and *in situ* secular equilibrium chlorine-36/chlorine (^{36}Cl/Cl) ratios for rock types of average composition, eastern Snake River Plain aquifer.

[U, uranium; Th, thorium; ppm, parts per million by weight; cm^2/g, square centimeters per gram; Δ, the values for the Snake River Plain shale represent only one sample and are not an average; *, data not available from Parker (1967)]

Rock type	Number of samples	U content (ppm)	Th content (ppm)	Thermal neutron cross section (cm^2/g)	Total neutron production rate (neutrons/ gram of rock/ year)	*In situ* secular equilibrium ^{36}Cl/Cl ratio ($\times 10^{-15}$)
Basalt: Average composition, Snake River Plain, this study	7	1.14	3.03	0.0096	3.44	5.2
Basalt: Average composition from Parker (1967)	*	1.00	4.00	.0073	3.68	7.3
Rhyolite: Average composition, Snake River Plain, this study	9	5.96	24.1	.0081	19.64	33.3
Rhyolite: Average composition, from Parker for felsic granite (1967)	*	3.5	18	.0069	14.62	30.7
Carbonate: Average composition, Snake River Plain, this study	6	2.35	0.19	.0036	1.81	7.0
Carbonate: Average composition, from Parker (1967)	*	2.2	1.7	.0039	2.46	9.1
Δ Shale: Snake River Plain, this study	1	2.6	9.07	.0120	7.49	9.1
Shale: Average composition, from Parker (1967)	*	3.2	11.0	.0098	9.27	13.7
Quartzite: Average composition, Snake River Plain, this study	2	0.85	2.12	.0042	1.26	4.0
Quartzite: Average composition, from Parker for sandstone (1967)	*	.45	1.7	.0061	0.73	1.7

Table 8. Maximum calculated equilibrium chlorine-36 (^{36}Cl) and associated total chloride (Cl^-) concentrations in ground water from *in situ* production due to neutron activation of stable chlorine-35 for six rock types from the eastern Snake River Plain aquifer.

[Sample locations are shown on figure 1. Source of data: rock density data from Dobrin (1976); percent porosity from Freeze and Cherry (1979); rock chloride content from U.S. Geological Survey Isotope Laboratory except values marked with an asterisk (*), which are from Parker (1967, table 19, p. D13-D14); maximum measured chloride content of ground water from R.C. Bartholomay (U.S. Geological Survey, written commun., 2000). Cl, chlorine; atoms/L, atoms per liter; g/cm^3, grams per cubic centimeter; g/L, grams per liter; mg/kg, milligrams per kilogram; mg/L, milligrams per liter. See text for explanation of the total transfer of ^{36}Cl and Cl from rock to ground water and maximum corrected *in situ* ^{36}Cl contribution to ground water]

Sample identifier and rock type	Rock density (g/cm^3)	Percent porosity	Chloride content in rock (mg/kg)	Total transfer of ^{36}Cl from rock to ground water (atoms/L × 10^8)	Total transfer of Cl^- from rock to ground water (g/L)	Maximum ambient Cl^- content of ground water (mg/L)	Maximum corrected *in situ* ^{36}Cl contribution to ground water (atoms/L × 10^5)
Igneous							
SP-5, rhyolite	2.51	1	*240	326	60.24	10	54.2
SP-6, rhyolite	2.51	1	*240	329	60.24	10	54.5
SP-7, rhyolite	2.51	1	600	942	150.60	10	62.5
SP-8, rhyolite	2.51	1	700	1,210	175.70	10	69.1
SP-9, opal deposit in rhyolite	2.51	1	*10	11.2	2.51	10	44.7
SP-10, rhyolite	2.51	1	*240	360	60.24	10	59.8
SP-13, rhyolite	2.51	1	*240	334	60.24	10	55.4
SP-15, basalt	2.61	5	*50	1.98	2.61	10	7.59
SP-16, basalt	2.61	5	100	3.73	5.22	10	7.15
SP-17, rhyolite	2.51	1	*240	481	62.64	10	76.8
SP-18, basalt	2.61	5	*50	1.65	2.61	10	6.32
SP-19, basalt	2.61	5	100	2.90	5.22	10	5.56
SP-20, basalt	2.61	5	200	2.55	10.44	10	2.45
SP-21, basalt	2.61	5	200	18.4	10.44	10	17.7
SP-22, basalt	2.61	5	*50	4.03	2.61	10	15.5
SP-23, rhyolite	2.51	1	*240	358	62.64	10	57.1
Sedimentary							
SP-1, limestone	2.54	1	100	25.2	25.40	15	14.9
SP-2, limestone	2.54	1	200	65.0	50.80	15	19.2
SP-3, limestone	2.54	1	*150	55.4	38.10	15	21.8
SP-4, dolomite	2.7	1	400	27.6	101.60	15	4.08
SP-12, limestone	2.54	1	200	61.2	50.80	15	18.1
SP-25, shale	2.42	1	*3000	1,170	762.00	15	23.1
SP-26, limestone	2.54	1	*150	71.8	38.10	15	28.3
Metamorphic							
SP-11, quartzite	2.74	1	100	29.8	27.40	15	16.3
SP-24, quartzite	2.74	1	*10	0.712	2.74	15	3.90